

Immobilization and characterization of novel L-asparaginase variant using functionalized multi-walled carbon nanotube

M.Sc. Thesis

By
SUKANYA SAMANTA

ROLL NO: 2203171019



**DEPARTMENT OF BIOSCIENCES AND BIOMEDICAL
ENGINEERING
INDIAN INSTITUTE OF TECHNOLOGY INDORE**

MAY 2024

Immobilization and characterization of novel L-asparaginase variant using functionalized multi-walled carbon nanotube

A THESIS

*Submitted in partial fulfillment of the
requirements for the award of the degree
of
Master of Science*

by
SUKANYA SAMANTA



**DEPARTMENT OF BIOSCIENCES AND BIOMEDICAL
ENGINEERING
INDIAN INSTITUTE OF TECHNOLOGY
INDORE
MAY 2024**



INDIAN INSTITUTE OF TECHNOLOGY INDORE

CANDIDATE'S DECLARATION

I hereby certify that the work which is being presented in the thesis entitled **Immobilization and Characterization of Novel L-asparaginase Variant using Functionalized Multi-walled Carbon Nanotube** in the partial fulfillment of the requirements for the award of the degree of **MASTER OF SCIENCE** and submitted in the **DEPARTMENT OF BIOSCIENCES AND BIOMEDICAL ENGINEERING, Indian Institute of Technology Indore**, is an authentic record of my own work carried out during the time period from July'2022 to May'2024 under the supervision of **Prof. Avinash Sonawane**, Supervisor of M.Sc. thesis.

The matter presented in this thesis has not been submitted by me for the award of any other degree of this or any other institute.

Sukanya Samanta 22.05.24
Signature of the student with date
SUKANYA SAMANTA

This is to certify that the above statement made by the candidate is correct to the best of my/our knowledge.

Signature of the Supervisor of M.Sc. Thesis
Prof. Avinash Sonawane

SUKANYA SAMANTA has successfully given his/her M.Sc. Oral Examination held on **10.5.2024**.

Signature of Supervisor of
M.Sc. Thesis
Date: **22.05.2024**

P.V. Kodgire
Convener, DPGC
Date: **22/05/24**

ACKNOWLEDGEMENTS

Firstly, I would want to give all praise and thanksgiving to the Almighty God, who gave me the courage to finish my thesis despite several obstacles. Occasionally, with never-ending experimentation, I got too disappointed. I developed the fortitude and perseverance to handle the unfavorable outcomes as the days went by. My confidence and enthusiasm increased as I carried out more experiments and saw excellent outcomes. With each new study, my interest in the subject matter grew significantly. I have developed several special traits as a result of finishing my current thesis study. I gained the ability to take on fresh challenges, solve issues, and approach my profession with renewed vigor every day. Think that each day is fresh, and my experiments will be no different. This cannot happen in the absence of the constant This won't be possible without the consistent suggestions of many people who played a vital role in completing this present thesis work.

I am profoundly indebted to my supervisor, **Prof. Avinash Sonawane**, whose steadfast guidance, unwavering support, and boundless expertise have been the cornerstones of this thesis. Their mentorship has not only shaped the trajectory of my research but also nurtured my growth as a scholar. I am truly grateful for their patience, encouragement, and insightful feedback, which have continuously inspired me to strive for excellence.

I would also like to thank **Prof. Suman Mukhopadhyay**, Department of Chemistry, IIT Indore, for his support and collaboration. I would also like to thank the Director, **Prof. Suhas Joshi**, for letting me be a part of such a prestigious institute. I want to thank **Prof. Amit Kumar** (Head, Department of Biosciences and Biomedical Engineering), **Prof. Prashant Kodgire** (Convener, DPGC), and **Dr. Parimal Kar** (M.Sc. Coordinator) for their suggestions throughout my M.Sc. journey. I would also like to express my humble thanks to all the faculty members of BSBE who taught me various courses during my coursework and constantly motivated me to bring better in me. I also like to thank the

Department of Biosciences and Biomedical Engineering (BSBE), the Indian Institute of Technology Indore, for providing a shear platform for me to pursue my research interest without any difficulties and for aiding in every possible way during this process.

My special thanks to **Bhagyashri Soumya Nayak** and **Sayantana Sarkar** for guiding and helping me out during the experiments. I want to thank him for his guidance at every point in time when I required some experienced insights from him.

I want to express my sincere thanks to all other lab members **Satyam Singh, Kishan Khandelwal, Birupakshya Pradhan, Suchi Chaturvedi, Sibi Karthik, Barsa Nayak, Priya Ghosh, Dhvani and Bidisha**, who are a source of learning and constant motivation during my project. I also want to thank each of them for providing a lab environment that taught me a lot. It will surely help me in my future endeavors.

To my friends, **Moumita Pal, Mallar Dasgupta, Swagata Lakshmi Dhali, Aritra Chakrabarty, Sampurna Dasgupta, Sugato Panda**, whose camaraderie, encouragement, and shared experiences have been a constant source of inspiration and solidarity, I extend my sincere gratitude. Your support, understanding, and collaborative spirit have enriched my academic journey immeasurably, and I am privileged to have had the opportunity to learn and grow alongside such exceptional individuals.

Finally, to my beloved family, whose boundless love, unwavering belief, and selfless sacrifices have been the cornerstone of my academic pursuit, I owe an immeasurable debt of gratitude. Your enduring encouragement, sacrifices, and unwavering faith in my abilities have been my source of strength and motivation, sustaining me through the challenges and triumphs of this journey

DEDICATION

I would like to dedicate my M.Sc. thesis to my mother.

ABSTRACT

L-asparaginase is an integral part of a multi-agent chemotherapy regimen for Acute Lymphoblastic Leukemia (ALL). The development of anti-asparaginase antibodies and safety concerns limit the use of *Escherichia coli* L-asparaginase (EcA), an essential component of multi-agent chemotherapy treatments for ALL. Our lab has developed L-asparaginase variants that show high activity, high stability, negligible glutaminase activity, and low immunogenicity in BALB/c mice and ALL patients. However, their half-life is still less due to degradation by proteases like Cathepsin B and Asparaginyl endopeptidase. Enzyme immobilization can decrease their degradation by proteases. Multi-walled carbon nanotubes (MWCNTs) exhibited a promising immobilization yield of 95.87% upon immobilization onto these functionalized MWCNTs (f-MWCNTs), which were activated using EDC and NHS after being functionalized with carboxyl groups. SEM, TEM, TGA, FT-IR, and Raman Spectroscopy were among the analytical methods used to validate the effective immobilization of L-asparaginase on the surface of the f-MWCNT. Compared to free enzymes, immobilized enzymes demonstrated superior kinetic characteristics at 37 °C, stability at both 37 °C and 62 °C, stability in PBS and human serum, and improved pH stability. Additionally, they showed reduced stability and antigenicity when exposed to proteases such as Asparaginyl endopeptidase and Cathepsin B. Furthermore, compared to free enzymes, immobilized enzymes showed higher efficacy in killing HeLa and MOLT-4 cells; this could be because the enzyme was released over an extended period or underwent less degradation. These results raise the possibility of creating novel, chemically modified L-asparaginase nano-bioconjugate with fewer side effects. These drugs could lead to better treatment outcomes and become a routine treatment for many diseases, including ALL.

LIST OF PUBLICATIONS

- Nayak B., Samanta S., Sonawane A., *Current insights and advancements in L-asparaginase-based therapeutic strategies for treating acute lymphoblastic leukemia* (Manuscript under preparation)
- Samanta S., Nayak B., Sarkar S., Sonawane A., Mukhopadhyay S., *Cancer-targeted functionalized Multi-walled Carbon nanotubes as carriers of L-asparaginase to achieve enhanced anti-cancer efficacy* (Manuscript under preparation)

TABLE OF CONTENTS

LIST OF FIGURES.....	xv
LIST OF TABLES.....	xix
NOMENCLATURE.....	xxi
ACRONYMS.....	xxiii
Chapter 1: Introduction.....	1
1.1 Leukemia and its types.....	1
1.2 Acute Lymphoblastic Leukemia (ALL).....	2
1.3 Diagnosis of ALL.....	3
1.4 Treatment of ALL.....	5
1.5 Role of L-asparaginase in the treatment of ALL.....	6
Chapter 2: Literature Review	10
Chapter 3: Objectives and experimental workflow.....	15
Chapter 4: Materials and Methodology.....	17
4.1 Materials.....	17
4.1.1 Strains.....	17
4.1.2 Chemicals.....	17
4.2 Methodology.....	17
4.2.1 Isolation and purification of wild-type L-asparaginase and its variants.....	17
4.2.1.1 Plasmid isolation of wild-type L-asp and its variants from <i>E. coli</i>	17
4.2.1.2 Preparation of BL21(DE3) competent cells using Calcium chloride (CaCl ₂) method.....	18
4.2.1.3 Transformation of isolated plasmids into BL21(DE3) competent cells.....	18
4.2.1.4 Isolation of L-asparaginase	19
4.2.1.5 Ammonium sulphate precipitation and dialysis.....	19

4.2.1.6	Purification of L-asparaginase protein by anion-exchange and size-exclusion chromatography	20
4.3	Characterization of purified wild-type L-asparaginase and its variants.....	20
4.3.1	Determination of protein concentration using the Bradford Method.....	20
4.4	Functionalization of Multiwalled Carbon nanotube.....	20
4.5	Immobilization of L-asparaginase onto functionalized MWCNT.....	21
4.6	Immobilization of L-asparaginase onto functionalized MWCNT.....	21
4.7	Immobilization Yield Determination.....	21
4.8	Biophysical Characterization of immobilized f-MWCNT.....	23
4.8.1	Scanning Electron Microscopy.....	23
4.8.2	Transmission Electron Microscopy.....	23
4.8.3	Thermogravimetric analysis (TGA).....	24
4.8.4	Fourier Transform Infrared Spectroscopy (FT-IR).....	24
4.8.5	Raman Spectroscopy.....	24
4.9	Biochemical characterization of immobilized f-MWCNT.....	24
4.9.1	Enzyme Kinetics.....	24
4.9.2	pH Stability.....	25
4.9.3	Stability in PBS and Human Serum.....	25
4.10	Protease Degradation.....	25
4.11	<i>In-vitro</i> Antigenicity.....	26
4.12	Cell Viability	26
	Chapter 5: Results and Discussion.....	29

Chapter 6: Conclusions and Scope for Future Work.....	53
REFERENCES.....	55

LIST OF FIGURES

Fig 1.1: Difference between normal blood cells and leukemic cells...	1
Fig 1.2: Origin of AML and ALL.....	3
Fig 1.3: Different diagnostic procedures for ALL.....	4
Fig 1.4: Steps of Chemotherapy Treatment of ALL.....	6
Fig 1.5: History and revolution of L-asparaginase.....	7
Fig 1.6: Structure of E. coli L-asparaginase.....	7
Fig 1.7: Role of L-asparaginase to prevent ALL.....	8
Fig 2.1: Side-effects of commercially available L-asparaginase drugs.....	10
Fig 2.2: Pitfalls of currently available L-asparaginase variants.....	11
Fig 2.3: Preparation of MWCNT-COOH and immobilization of L- asparaginase.....	12
Fig 2.4: EDC-NHS Coupling reaction.....	13
Fig 3.1: Experimental strategy.....	15
Fig 5.1: (A) 0.8% Agarose gel image of isolated wild-type and Mut C Plasmid.....	29
(B) 0.8% Agarose gel image of restriction digested plasmid.....	29
Fig 5.2: (A) Transformed colonies of Mut C-pET28a-BL21(DE3)....	30
(B) Transformed colonies of Wildtype-pET28a-BL21(DE3).....	30
Fig 5.3: (A) 12% SDS-PAGE of isolated protein from transformed colonies of WT-pET28a-BL21(DE3).....	31
(B) 12% SDS-PAGE of isolated protein from transformed colonies of Mut C-pET28a-BL21(DE3).....	31
Fig 5.4: (A) Streaked plate of WT-pET28a-BL21(DE3) from colony 3.....	31
(B) Streaked plate of Mut C-pET28a-BL21(DE3) from colony 1.....	31

Fig 5.5: (A) 100x microscopic image after Gram-staining of WT-pET28a-BL21(DE3).....	31
(B) 100x microscopic image after Gram-staining of Mut C-pET28a-BL21(DE3).....	31
Fig 5.6: (A) 12% SDS-PAGE image of wild-type crude protein after 1,2,3,4,5,6 hour of IPTG induction.....	32
(B) 12% SDS-PAGE image of Mut C crude protein after 1,2,3,4,5,6 hours of IPTG induction, PI: Post induction.....	32
Fig 5.7: (A) Wild-type L-asp purification by ammonium sulphate precipitation and dialysis.....	33
(B) Mut C L-asp purification by ammonium sulphate precipitation and dialysis.....	33
Fig 5.8: (A) Wild-type L-asp purification by anion-exchange and size-exclusion chromatography.....	34
(B) Mut C L-asp purification by anion-exchange and size-exclusion chromatography.....	34
Fig 5.9: (A) Chromatogram of purified Wild-type L-asparaginase protein by anion-exchange chromatography.....	34
(B) Chromatogram of purified Mut C L-asparaginase protein by anion-exchange chromatography.....	34
(C) Chromatogram of purified Wild-type L-asparaginase protein by size-exclusion chromatography.....	35
(D) Chromatogram of purified Mut C L-asparaginase protein by size-exclusion chromatography.....	35
Fig 5.10: (A) 12% SDS-PAGE of Mut C L-asparaginase after purification by anion-exchange and size-exclusion chromatography..	35
(B) 12% SDS-PAGE of wild-type L-asparaginase after purification by anion-exchange and size-exclusion chromatography.....	36

Fig 5.11: BSA Standard curve.....	37
Fig 5.12: Effect of L-asparaginase concentration on immobilization yield.....	38
Fig 5.13: Effect of ASNase concentration on immobilization yield....	39
Fig 5.14: (A) SEM image of MWCNT.....	40
(B) SEM image of f-MWCNT.....	40
(C) SEM image of immobilized f-MWCNT.....	40
Fig 5.15: (A)TEM image of MWCNT.....	41
(B) TEM image of immobilized f-MWCNT.....	41
Fig 5.16: TGA Analysis of MWCNT- Before and after immobilization.....	42
Fig 5.17: FT-IR Spectra of MWCNT- Before and after immobilization.....	43
Fig 5.18: Raman spectra of MWCNT and immobilized MWCNT.....	44
Fig 5.19: (A) Velocity vs substrate concentration plot for free and immobilized enzymes at 37°C.....	45
(B) Velocity vs substrate concentration plot for free and immobilized enzymes at 62°C.....	45
Fig 5.20: (A) Kcat % of free and immobilized enzyme at 37°C.....	46
(B) Kcat % of the free and immobilized enzyme at 62°C.....	46
Fig 5.21: pH stability of free and immobilized enzymes.....	47
Fig 5.22: (A)PBS Stability profile of the free and immobilized enzyme.....	48
(B) Serum Stability profile of the free and immobilized enzyme.....	48
Fig 5.23: (A) Degradation study of Free and Immobilized L-asparaginase using Acetyl Endopeptidase (AEP).....	49

(B) Degradation study of Free and Immobilized L-asparaginase using Cathepsin B (CTSB).....49

Fig 5.24: The *in-vitro* antigenicity of free v/s immobilized L-asparaginase was determined by indirect ELISA50

Fig 5.25: (A) Cell viability of HeLa cells cultured with untreated MWCNT and functionalized MWCNT of different concentrations after 24 hours.....51

(B) Cell viability of HeLa cells cultured with free and immobilized enzymes of different activity ranges.51

Fig 5.26: Cell viability of MOLT-4 cells cultured with free and immobilized enzymes of different activity ranges.....52

LIST OF TABLES

Table 5.1: Spectrophotometric analysis of isolated plasmid DNA.....	29
Table 5.2: Concentrations of pure-proteins.....	37
Table 5.3: Immobilization yield at different concentrations of L-asparaginase.....	38
Table 5.4: Immobilization yield at different concentrations of L- asparaginase.....	39
Table 5.5: The kinetic parameters for each enzyme at 37 °C.....	46
Table 5.6: The kinetic parameters for each enzyme at 62 °C.....	46

NOMENCLATURE

IPTG: Isopropyl 1- β -D thiogalactopyranoside

NHS: N-hydroxy succinimide

EDC: 1-ethyl-3-(3-dimethyl aminopropyl) carbodiimide

AIBN: Azobisisobutyronitrile

TMB: 3,3',5,5'-Tetramethylbenzidine

TCA: Trichloroacetic acid

MTT: 3-[4,5-dimethylthiazol-2-yl]-2,5 diphenyl tetrazolium bromide

WST-8: 2-(2-methoxy-4-nitrophenyl)-3-(4-nitrophenyl)-5-(2,4-disulfophenyl)-2H-tetrazolium, monosodium salt

ACRONYMS

ALL: Acute Lymphoblastic Leukemia

AML: Acute Myeloblastic Leukemia

CLL: Chronic Lymphoblastic Leukemia

CML: Chronic Myeloblastic Leukemia

CBC: Complete Blood Count

SWCNT: Single-walled Carbon Nanotube

MWCNT: Multiwalled Carbon Nanotube

PMMA: Poly methyl methacrylate

MMA: Methyl methacrylate

AA: Acrylic acid

GMA: Glycidyl Methacrylate

SDS: Sodium Dodecyl Sulphate

PAGE: Polyacrylamide Gel Electrophoresis

AHA: Aspartic Acid beta-hydroxamate

PEG: Polyethylene Glycol

SEM: Scanning Electron Microscopy

TEM: Transmission Electron Microscopy

TGA: Thermogravimetric Analysis

FT-IR: Fourier Transform Infrared Spectroscopy

PBS: Phosphate Buffer Saline

AEP: Asparaginyl Peptidase

CTSB: Cathepsin B

ELISA: Enzyme-linked immunosorbent assay

CV: Column Volume

RRA: Relative Recovery of Activity

IE: Immobilization efficiency

RPMI: Roswell Park Memorial Institute

DMEM: Dulbecco's Modified Eagle Medium

CCK: Cell Counting Kit

ADA: Anti-drug Antibody

CHAPTER 1

Introduction

1.1 Leukemia and its types

Leukemia is an uncontrolled proliferation of immature blood cells that are in their early stage of development, also known as blast cells. Blood-forming tissues in humans, like bone marrow and lymphatic systems, are mostly affected by leukemia. Leukemia leads to the production of abnormal white blood cells (WBCs), which crowd out normal blood cells like erythrocytes and platelets, impairing the body's ability to fight infections and control bleeding.

According to the report submitted by the National Institute of Health in 2023, there are 6540 new cases of Acute Lymphoblastic Leukemia (ALL) in the world which is 0.3% of all cancers. The number of deaths is 1390, which is 0.2% of deaths by cancer.¹ Though the number of cases is less in comparison to other types of cancers, research is still necessary to discover better treatment options due to the severity of the disease and the limitations of current treatments.

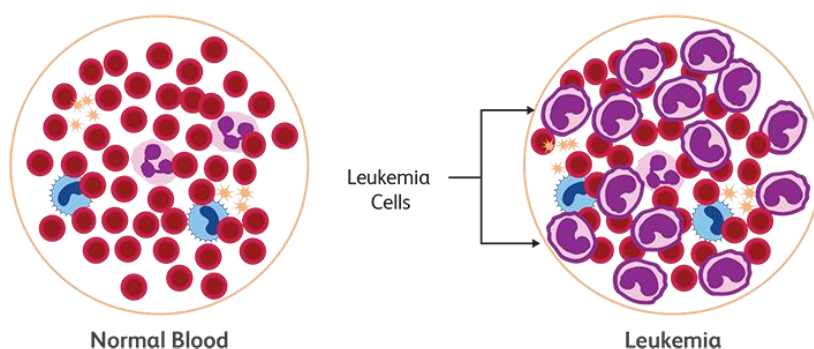


Fig 1.1: Difference between normal blood cells and leukemic cells
Ref: <https://www.bdbiosciences.com/enus/learn/clinical/blood-cancers/leukemia>

Leukemia can be broadly categorized into two main types: Acute and Chronic. Acute leukemia is the rapid proliferation of immature white

blood cells. Due to its rapid progression, it requires prompt treatment. Chronic leukemia progresses at a much slower rate than acute leukemia. Proliferation of mature but abnormal white blood cells occurs in the case of chronic leukemia. Initially, it may not show any symptoms, so treatment is not required in the early stages for some patients.

Acute and Chronic Leukemia can be further subdivided into four types:

- **Acute lymphoblastic Leukemia (ALL):** Uncontrolled proliferation of undifferentiated lymphoblast cells which is the precursor of Band T Lymphocytes. It is more common in children than adults.
- **Acute Myeloblastic Leukemia (AML):** Uncontrolled proliferation of undifferentiated myeloblast cells which is the precursor of monocytes and granulocytes like neutrophils, eosinophils, and basophils.
- **Chronic Lymphocytic Leukemia (CLL):** Uncontrolled proliferation of lymphoblast cells but progresses at a much slower rate than ALL.
- **Chronic Myeloblastic Leukemia (CML):** Uncontrolled proliferation of myeloblast cells but progresses slower than AML.

1.2 Acute Lymphoblastic Leukemia (ALL)

Invasion of blood, bone marrow, and extramedullary locations by immature lymphoid cells that are in an early stage of development is known as ALL. In the case of ALL, Lymphoblast cells cannot differentiate into B and T cells and proliferate uncontrollably. There are mainly three types of ALL: B Cell ALL, T Cell ALL, and Philadelphia positive ALL.² Children (1–14 years), young adults (15–39 years), and older individuals (>39 years) are the three age ranges in which ALL may manifest. Though the pediatric or children ALL is most common, it is curable in most cases, whereas the number of deaths is higher in adult cases.²

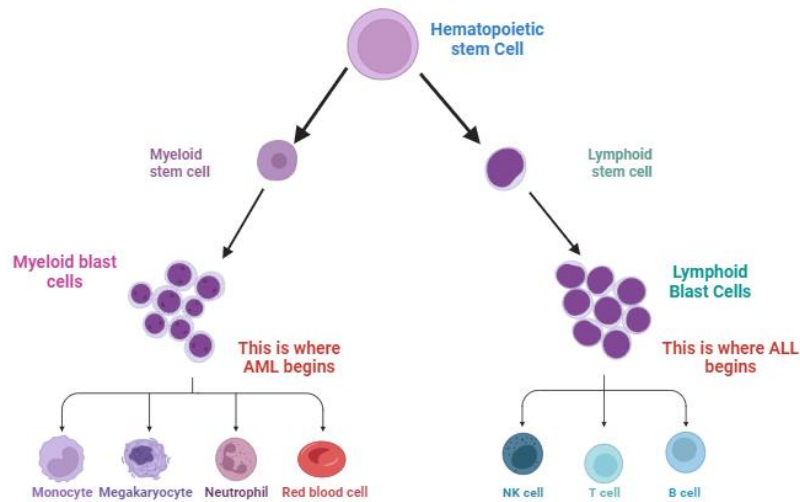


Fig 1.2: Origin of AML and ALL

The common symptoms of ALL are petechiae or small red spots on the skin, bleeding tendency, night sweats, enlarged spleen, kidney, and liver, fatigue and fever, swollen lymph nodes, anemia, loss of weight, etc. There can be many underlying causes of ALL: it can be genetic because there are many genes involved in the differentiation of blood cells, and mutation on any of those genes can cause ALL. Predisposing factors can also be environmental, like Pesticide exposure, ionizing radiation, and childhood infection. Genetic disorders like Down syndrome and translocation of chromosomes can also cause ALL. Translocation between chromosomes 12 and 21 is more common in children ALL, and Philadelphia-positive ALL (between chromosomes 9 and 22) is more common in adults.^{3,4}

1.3 Diagnosis of Acute Lymphoblastic Leukemia

The common procedures that are used for diagnosis of ALL are:

- **Complete Blood Count (CBC):** In this diagnostic technique, blood is drawn from veins using a needle and checked under a microscope to get the count of different blood cells. The number of RBCs or erythrocytes, WBCs, and platelets are counted. In ALL, the number of immature blood cells increases, which

makes less space available for other blood cells. So, the number of RBCs and platelets is reduced which can be diagnosed by CBC.⁵

- **Peripheral blood smear:** In this method, blood is collected from the patient, a drop of blood is placed on the slide, and a smear is made with another slide and observed under the microscope. Differences in shape and structure of the white blood cells, majorly blast cells, can be observed.⁵
- **Blood chemistry studies:** Different chemicals or biomarkers are present in the blood that are overexpressed in the case of ALL. Blood samples can be checked for those biomarkers.⁶
- **Bone marrow aspiration and Biopsy:** A hollow needle is inserted in the breastbone or hipbone of the patient, and a small amount of blood, bone marrow, and bone is removed, which is observed under the microscope. Immature lymphoblast or myeloblast cells can be observed.⁵

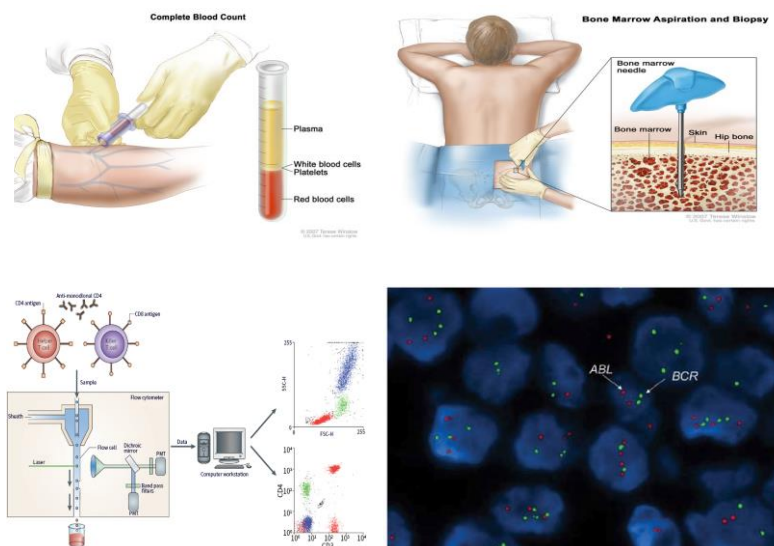


Fig 1.3: Different diagnostic procedures for ALL

Ref: <https://www.cancer.gov/types/leukemia/patient/adult-all-treatment-pdq>

- **Cytogenetic tests:** ALL is polygenic. Mutations in genes that are involved in blood cell proliferation and differentiation can cause ALL. If a patient has Down syndrome (Trisomy,21) he

or she is likely to develop ALL. Philadelphia chromosome (translocation between 9 and 22) is more common in adult ALL whereas translocation between 12 and 21 is more common in children. These changes can be observed by the cytogenetics tests in the laboratory using blood or bone marrow samples.^{5,6}

- **Immunophenotyping:** Immunophenotyping can be performed to identify specific markers present on the blast cell surface. Specific antibodies tagged with fluorescent dyes are used and flow cytometry assay is performed. It can give an idea about the count of immature blood cells.⁶

1.4 Treatment of ALL

Chemotherapy and Radiation therapy are commonly used to treat Acute lymphoblastic leukemia. Chemotherapy involves four stages:

1. Induction: Induction chemotherapy aims to eradicate the disease burden and achieve normal hematopoiesis by using a combination of drugs like Glucocorticoid, vincristine, L-asparaginase, Anthracycline,² etc.

2. Consolidation: The second part of chemotherapy treatment is consolidation which consists of several sequential short courses in two weeks with Glucocorticoid, a high dose of methotrexate, low-dose cytarabine, and L-asparaginase.

3. Intensification or reinduction: The consolidation step is followed by intensification or reinduction therapy, in which the same drugs are used as the induction step.

4. Maintenance: The maintenance step is to prevent the recurrence of disease that involves using drugs like Mercaptopurine, Glucocorticoid, Methotrexate, Vincristine, etc.

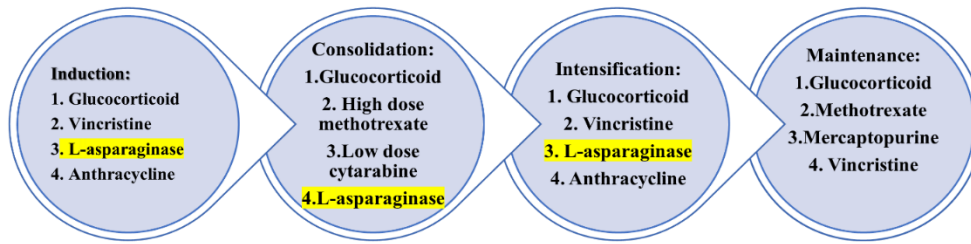


Fig 1.4: Steps of Chemotherapy Treatment of ALL

Nowadays, intrathecal chemotherapy, chemotherapy with stem cell transplant, targeted therapy using monoclonal antibody, and Chimeric Antigen Receptors-T Cell therapy are also used to treat ALL.³

1.5 Role of L-asparaginase in the treatment of ALL

L-asparaginase is one of the main chemotherapeutic agents used to treat ALL as well as other malignant conditions like Hodgkin's disease, various forms of lymphoma, and sarcoma, as is evident. L-asparaginase activity was first seen in cow tissues by Lang. In 1953 Kidd found the inhibition of lymphosarcoma by L-asparaginase isolated from pig serum.⁷ In 1956, Robert and co-workers isolated two forms of *E. coli* asparaginase: Type I and Type II. The Km of type II asparaginase is lesser than that of Type I. So, Type II asparaginase of *E. coli* is mostly used in therapeutics. PEGylated L-asparaginase and *Erwinia chrysanthami* derived L-asparaginase are currently extensively used in treatments due to their longer half-lives and decreased immunogenicity, respectively.^{7,8}

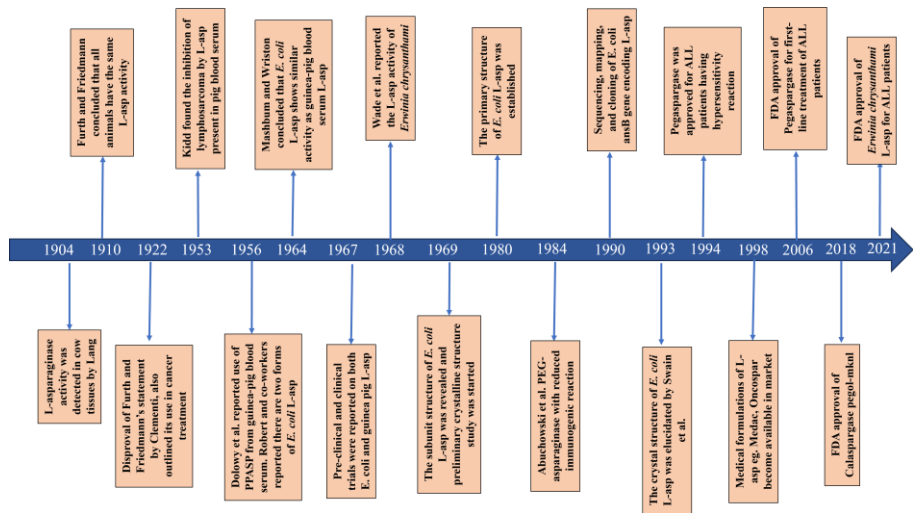


Fig 1.5: History and revolution of L-asparaginase

The homo-tetramer L-asparaginase Type II derived from *E. coli* has a molecular weight of 139 kDa. There are four subunits: A, B, C, and D. The molecular weight of each subunit is 34.6 kDa. The structure is properly called a dimer of dimers formed by A-C and B-D subunits. There is a 327 amino acid-long active site lying between the interface of these dimers. Each active site is shaped by the haulage of amino acids arranged in two adjacent monomers.^{9,10,11}

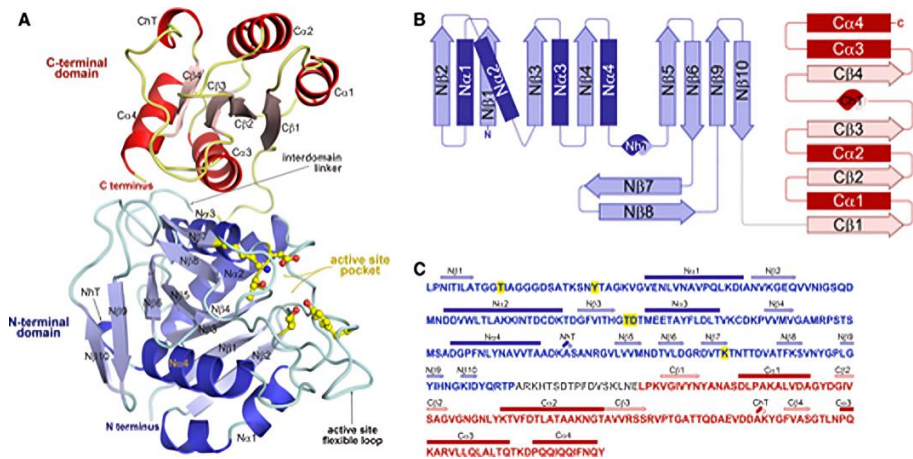


Fig 1.6: Structure of *E. coli* L-asparaginase

L-asparaginase acts by shutting down the metabolism of neoplastic leukemic cells. The malignant leukemic cells lack an enzyme named Asparagine synthetase which is important for the biosynthesis of asparagine. Therefore, these cells depend on blood L-asparagine for protein synthesis. The enzyme L-asparaginase is an amidohydrolase

that converts L-asparagine to L-aspartate and ammonia, thereby depleting asparagine from the blood, which leads to activation of the apoptosis pathway in the leukemic cells and eventually, they undergo apoptosis.²

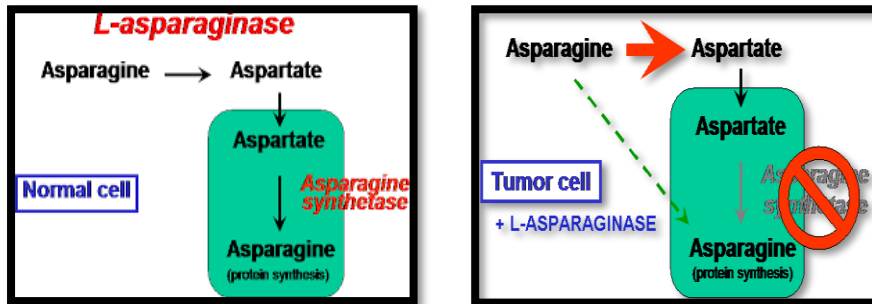


Fig 1.7: Role of L-asparaginase to prevent ALL

At present, numerous clinical data strongly support the use of asparaginase for the therapy of pediatric ALL. Though the intensive asparaginase treatment is more beneficial than the less intensive one^{12,3}, it has some side effects due to its glutaminase activity and bacterial origin (isolated from *E. coli*). Hepatotoxicity and neuro-toxicity are some adverse effects of glutaminase activity of L-asparaginase. There is an ongoing debate among scientists about whether glutaminase activity is required or not for killing cancer cells. Some scientists proposed glutaminase activity is required only in Asparaginase synthetase positive cells not in Asparaginase synthetase negative cancer cells.^{13,14} Pancreatitis, Hyperglycemia, Triglyceridemia, and Thrombosis are some other side effects of using asparaginase as a chemotherapy drug. Since asparaginase is identified as foreign by the human immune system, the formation of anti-drug antibodies also neutralizes the enzyme activity through the silent inactivation process. In addition to this, *E. coli* asparaginase administration induces undesired side effects in many patients, including severe allergic reactions. Due to its bacterial origin, it can also cause hypersensitivity reactions in some patients. Also, some proteases and endopeptidases degrade L-asparaginase in blood, reducing their *in-vivo* half-life. Due to these adverse effects of asparaginase, there is a vigor need to have an ASNase-based therapy with lesser side effects and better efficacy.¹⁵

Chapter 2

Literature review

L-asparaginase, despite being a major chemotherapy drug in the treatment of ALL, has several side effects due to its large structure, bacterial origin, and secondary glutaminase activity. Hypersensitivity, hepatotoxicity, neurotoxicity, hyperglycemia, thrombosis, and pancreatitis are the major side effects observed in children and adult ALL patients, and managing these toxicities is challenging for many adult and pediatric oncologists.¹⁵

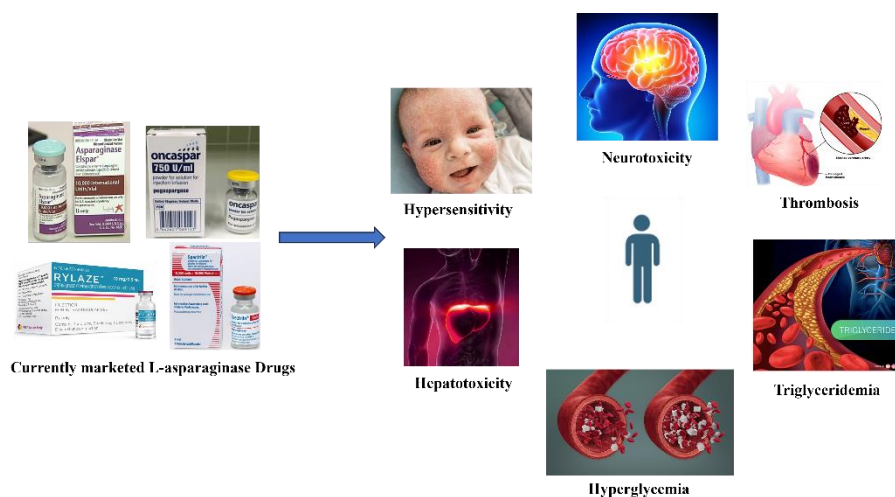


Fig 2.1: Side-effects of commercially available L-asparaginase drugs

To reduce the side-effects of commercially available L-asparaginase, our lab has used rationale protein engineering techniques and created variants of *E. coli* L-asparaginase II. Specific amino acids are substituted by another amino acid using a PCR-based site-directed mutagenesis method to produce L-asp variants that show high activity, high stability, negligible glutaminase activity, and low immunogenicity in BALB/c mice and ALL patients. Their binding affinity with Anti-asparaginase antibodies is lesser than the binding affinity of wild-type L-asp, which reduces the silent inactivation. None of them are found

toxic *in vivo* and they showed significantly improved efficacy in animal leukemia models.¹⁶

However, some proteolytic enzymes like cathepsin and acetyl endopeptidase cleave the L-asparaginase, thus reducing their *in-vivo* half-life and activity. Therefore, further modifications are needed to increase their dosage frequency to get optimum efficacy. Nano formulations of L-asparaginase can be helpful to overcome these problems. Nano-encapsulation or immobilization masks the recognition sites of L-asparaginase, which are recognized by antibodies and reduce hypersensitivity and silent inactivation, preventing degradation by proteases like Cathepsin B, Asparaginase endopeptidases thus improving *in-vitro* and *in-vivo* stability of the drug, increases half-life.¹²

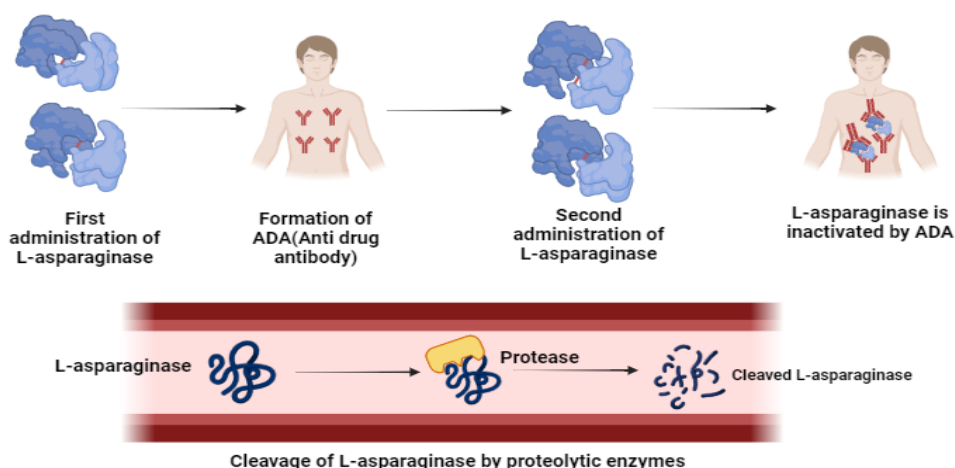


Fig 2.2: Pitfalls of currently available L-asparaginase

Many scientists have encapsulated or immobilized asparaginase to increase its stability and *in vivo* half-life using a variety of materials like silk, PLGA, silica, magnetic nanoparticles, liposomes, polymersomes, Hollow nanospheres, polyion vesicles, hydrogels, virus-like particles, RBC, etc. Each method of immobilization has some advantages and disadvantages. For example, the synthesis of liposomes is easy and cheap, but it is not stable and has reduced blood circulation times. Biopolymers are biodegradable but have heterogeneity in size and poor mechanical properties. Magnetic nanoparticles and

polymerosomes are not often biodegradable, whereas hollow nanoparticles and polyion vesicles are poorly studied.¹⁷

In this project, we have tried to use Polymethyl methacrylate and its copolymers with acrylic acid and Glycidyl methacrylate for immobilization of L-asparaginase. Polymethyl methacrylate (PMMA) is easy to synthesize, cheap, easily scalable, biocompatible, and it has been used for drug delivery with a good toxicological safety report. But it has low biodegradability.¹⁸ To increase its biodegradability copolymer formation with a biodegradable polymer can be beneficial.¹⁹ Acrylic acid (AA) is a biodegradable polymer, so the copolymer of methyl methacrylate (MMA) and AA should have increased biodegradability.²⁰ Also, the reactivity of MMA is greater than AA. MMA will form the core of the particle, and more AA is expected on the surface, which will help in protein immobilization. The Glycidyl methacrylate (GMA) contains an epoxy group that can be easily modified to become vicinal diols, amines, or aldehyde groups, which helps in the immobilization of enzymes and proteins.²¹ Therefore, the copolymers of Methyl methacrylate with acrylic acid and glycidyl methacrylate will help in increasing its biodegradability and better immobilization of L-asparaginase.

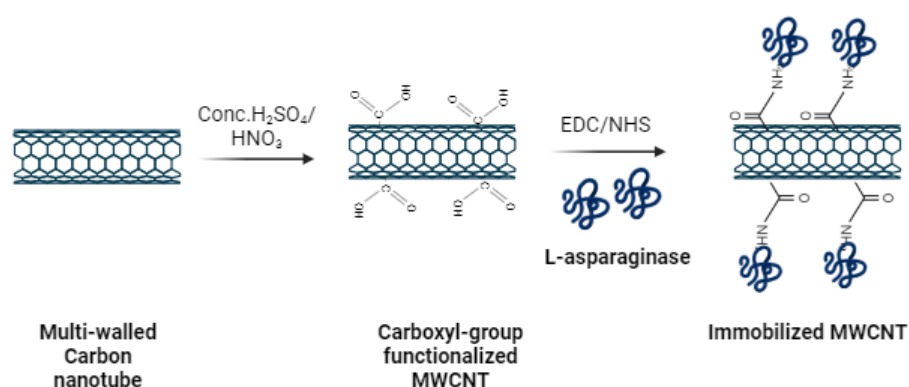


Fig 2.3: Preparation of MWCNT-COOH and immobilization of L-asparaginase

Simultaneously, we used COOH-functionalized multi-walled carbon Nanotubes (MWCNT) treated with 1-Ethyl-3-(3-dimethylaminopropyl) carbodiimide Hydrochloride and N-hydroxysuccinimide (NHS) for immobilizing our novel L-asparaginase. MWCNTs hold promise in drug delivery applications due to their unique properties. With a high surface area, MWCNTs enable efficient drug loading, and their biocompatibility can be enhanced through surface modifications. Functionalization with various molecules allows customization for specific drug delivery needs, providing protection against degradation and allowing controlled release.²² The most common modification is oxidation of MWCNT using sulfuric acid or nitric acid. In previous studies, commercialized L-asparaginase was immobilized onto the surface of MWCNT and COOH-functionalized MWCNT which showed high immobilization yield (IY) and high relative recovery activity (RRA). The nano-bioconjugate also showed high stability and retained its activity after some consecutive reaction cycles.²³

Coupling agents such as NHS (N-hydroxysuccinimide) and EDC (1-ethyl-3-(3-dimethylaminopropyl) carbodiimide) are frequently employed to immobilize proteins onto nanoparticles. In this process, EDC activates the carboxylic acid groups on the surface of the nanoparticles, resulting in the formation of an O-acylisourea intermediate. After that, NHS is added to this intermediate to stabilize it and produce a stable NHS-ester.

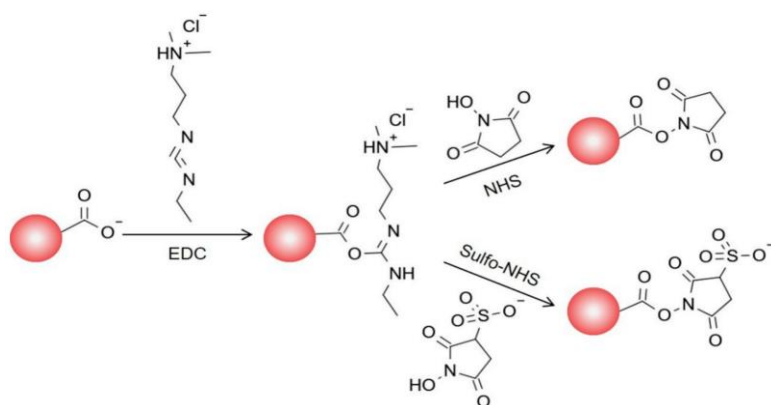


Fig 2.4: EDC-NHS Coupling reaction (*Ref:* www.mdpi.com)

Strong and long-lasting amide connections can be formed between amino groups on proteins and the activated groups on the surface of nanoparticles through a covalent interaction. In comparison to physical adsorption techniques, this covalent connection decreases non-specific binding and provides improved stability. Because of its versatility and applicability to different proteins and nanoparticles, EDC/NHS coupling is frequently employed in biomedical applications, such as medication administration and diagnostics.²⁴

Chapter 3

Objectives and Experimental Work Flow

1. Isolation and purification of wild-type L-asparaginase and its variant
2. Characterization of purified wild-type L-asparaginase and its variant
3. Functionalization of Multiwalled Carbon nanotube and immobilization of L-asparaginase variant
4. Characterization study of immobilized L-asparaginase
5. Cytotoxicity assessment in ALL Cell line

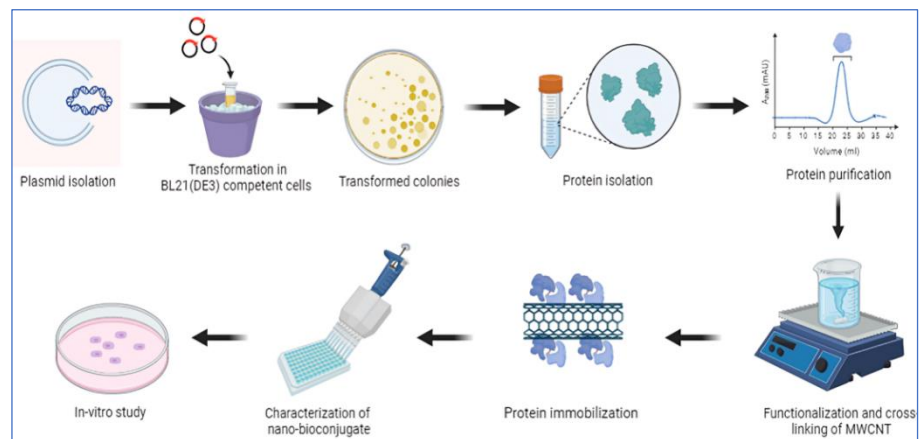


Fig 3.1: Experimental strategy

CHAPTER 4

Materials and Methods

4.1 Materials

4.1.1 Strains

E. coli DH5 α (Kindly provided by Dr. Klaus Roehm, University of Marburg, Germany) and *E. coli* BL21 (DE3) (ATCC) are used throughout the study.

4.1.2 Chemicals

All chemicals used in the present study were of reagent grade and were purchased either from Merck (Darmstadt, Germany) or Sigma Aldrich (New Jersey, USA). The plasmid isolation kit was from QiaGen. All the reagents and solvents used in the project, SDS PAGE, were purchased from Sigma (New Jersey, USA), SRL (Mumbai, India), and Hi-Media (Mumbai, India). The chemicals were used as it is without any purifications or modifications. The antibiotics used for growing cultures were purchased from Sigma Aldrich (New Jersey, USA). The columns used for Anion exchange chromatography and size exclusion chromatography are the Hi-trap Q-HP Sepharose column and Superdex 200 Increase 10/300 GL high-resolution column from Cytiva, respectively (Marlborough, USA).

4.2 Methodology

4.2.1 Isolation and purification of wild-type L-asparaginase and its variants

4.2.1.1 Plasmid isolation and restriction digestion of wild-type L-asp and its variants from *E. coli*

E. coli cells containing the required plasmid were revived from 30% Glycerol stock in 3 ml LB Medium containing Kanamycin and Tetracycline by culturing it overnight at 37 °C at 220 r.p.m. Then,

subculturing was done in a 10 ml LB Medium containing antibiotics. After 12-14 hours, the culture was centrifuged at 13000 r.p.m for 2-3 minutes to get the pellet. The plasmid was then isolated using the Qiagen Miniprep Plasmid isolation kit by adding resuspension, lysis, and neutralization buffer respectively. Finally, the silica column was washed using wash buffer, and Plasmid was eluted using elution buffer. The plasmid concentration and purity were checked in nanodrop, and the size of the plasmid was checked using Agarose Gel Electrophoresis. The restriction digestion of the isolated plasmids of Mutant-C and Wild-type was performed using NEB (Ipswich, Australia) buffers and restriction enzymes. The isolated plasmids were added with the Cut Smart restriction buffer with *EcoRI* and *HindIII* restriction enzymes. The mixture was incubated at 37 °C for 90 minutes, and the resultant was run on 1% Agarose gel to obtain the band of the insert on the gel.

4.2.1.2 Preparation of BL21(DE3) competent cells using Calcium chloride (CaCl₂) method

Competent cells were prepared using the CaCl₂ solution. *E. coli* BL21(DE3) cells were grown overnight in 3ml media containing Tetracycline. After 12-14 hours, the cells were again subcultured in 10 ml LB Medium at 37 °C at 220 r.p.m until the OD reached 0.6. The culture was then centrifuged at 3000 r.p.m at 4 °C for 5 minutes. After washing the pellet with autoclaved Mili Q again centrifuge it at 8000 r.p.m for 5 minutes at 4 °C. Then, the pellet was washed with 0.1 M CaCl₂ and again centrifuged at 8000 r.p.m for 5mins at 4 °C. Finally, the pellet was dissolved in 500 µl 0.1 M CaCl₂.

4.2.1.3 Transformation of isolated plasmids into *E. coli* BL21(DE3) competent cells

Transformation of plasmid in *E. coli* BL21 cells was done using the heat shock method. 7 µl of Plasmid DNA was added to 100 µl of competent *E. coli* BL21(DE3) cells and kept on ice for 30 minutes. Then, the mixture was immediately transferred to a thermo-mixture and kept for 90 seconds. Immediately, the mixture was transferred to ice for

10 minutes. 1ml of LB Media was added to the mixture and kept at 37 °C for 1 hour. The mixture was then centrifuged at 3000 r.p.m for 5 minutes at room temperature. After discarding the supernatant, around 100 µl of the pellet was spread on LB Agar plates containing Kanamycin and Tetracycline and incubated at 37 °C overnight.

4.2.1.4 Isolation of L-asparaginase

Single transformed colonies were isolated from the agar plates and used to inoculate LB Broth containing Kanamycin and Tetracycline and incubated for 12-14 hours at 37 °C at 220 r.p.m. Then, the secondary culture was prepared using that culture and incubated at 37 °C and 220 r.p.m until the OD reached 0.6. Then, the secondary culture was induced with 0.5 mM IPTG and incubated at 37 °C at 220 r.p.m for 4 hours. The culture was then centrifuged at 10000 r.p.m for 3 minutes. The pellet was then resuspended using a hypertonic buffer by vortexing and kept on ice for 10 minutes. The mixture was then centrifuged at 13000 r.p.m for 20 mins at 4 °C. After discarding the supernatant, the pellet was again dissolved in chilled autoclaved Mili Q by vortexing and kept on ice for another 10 mins. The mixture was then centrifuged at 13000 r.p.m for 25 mins, and supernatant that contained crude protein was stored at 4 °C.

4.2.1.5 Ammonium sulphate precipitation and dialysis

After the isolation of the crude protein, gradient ammonium sulphate precipitation is performed (50% and 90%). For 50% precipitation, the crude protein was placed on a magnetic stirrer at 4 °C for 90 mins, and ammonium sulphate was added gradually. Then, the protein was centrifuged at 13000 r.p.m for 20 minutes. Again for 90% precipitation, the supernatant was placed on a magnetic stirrer for 60 minutes and ammonium sulphate was subsequently added to it. The protein was then centrifuged at 13,500 r.p.m for 20 mins. The pellet was then resuspended into 50 mM Tris-HCl (pH = 8.5). The protein was then dialyzed overnight against Tris-HCl (pH = 8.5).

4.2.1.6 Purification of L-asparaginase protein by anion-exchange and size-exclusion chromatography

Chromatographic purification was performed using the AKTA Pure system. For anion-exchange chromatography, a Hi-trap Q-HP column from Cytiva was used, which has positively charged resins that help to bind and elute negatively charged L-asparaginase (as the pI of L-Asp is around 5). The column volume is 5 cv, and it was equilibrated with 50 mM Tris-HCl (pH = 8.5), and then the sample was injected and finally eluted in 50 mM Tris-HCl (pH = 8.5), 300 mM NaCl. The machine was set at method run, and the method was designed by putting 15 column volume (CV) and a flow rate of 0.5 ml/minute.

Additionally, gel filtration chromatography was used to obtain 100% pure protein. For the gel filtration chromatography, the Superdex 200 Increase 10/300 GL high-resolution column from Cytiva was utilized. The column volume is 2 cv, and it was equilibrated with 50 mM Tris-HCl (pH = 8.5), and then the sample was injected and finally eluted in 50 mM Tris-HCl (pH = 8.5), 300 mM NaCl. A flow rate of 0.5 ml/min was used. Every elution was acquired in a 1ml buffer.

4.3 Concentrating Pure Protein

The purified protein was concentrated using Sigma Amicon[®] Ultra 4 mL Centrifugal Filters (10kDa). First, the column was washed using autoclaved MiliQ and then equilibrated with 50 mM Tris-HCl (pH = 8.5). The protein was then added to the filter and centrifuged at 7000 r.p.m for 15 mins. The flowthrough was discarded, and the concentrated protein was collected in a microcentrifuge tube.

4.4 Characterization of purified wild-type L-asparaginase and its variant

4.4.1 Determination of protein concentration using the Bradford Method

For quantitative analysis of protein, Bradford Assay was performed. First, the standard curve was prepared using Bovine Serum Albumin at

different concentrations. Then, the protein samples were diluted 100 times. Then 80 μ l protein dilutions were added to 120 μ l of Bradford Reagent and incubated for 5 minutes at room temperature. Absorbance was taken at 595nm.

4.5 Functionalization of Multiwalled Carbon nanotube

Functionalization of the Multi-walled Carbon Nanotube was performed using a highly concentrated mixture of nitric acid and sulphuric acid, and the mixture was sonicated for 3 hours. Then, the mixture was centrifuged at 600 r.p.m for 30 minutes. Finally, the particles were washed and dried in a vacuum overnight. Crosslinking with EDC was performed by treating COOH functionalized MWCNT with 40 mg/L NHS and 20 mg/L EDC in phosphate buffer for 1 hour. The solution was then centrifuged at 20000 x g for 1 hour, and the supernatant was discarded. The pellet was then dried overnight in a vacuum.

4.6 Immobilization of L-asparaginase onto functionalized MWCNT

In a typical experiment, 2.0 ± 0.2 mg of functionalized MWCNT were treated with 200 μ l of L-asparaginase solution of increasing concentrations (0.25, 0.5, 0.75, and 1 mg/ml) respectively and stirred in an orbital shaker at 50 r.p.m for one hour. The solution was then centrifuged at 20000 r.p.m for 15 mins and the supernatant was collected for calculating immobilization yield and relative recovery of activity (RRA). For every condition, at least three separate tests were conducted, enabling the calculation of the relative recovered activity, average immobilization yield, and corresponding standard deviations.

4.7 Determination of immobilization efficiency

The immobilization yield of f-MWCNT was determined using two methods: (A) by the Bradford method and (B) by calculating the enzyme activity of the supernatant.

4.7.1 Bradford method

80 μ l of supernatant was collected and mixed with 120 μ l of Bradford reagent and incubated for 5 minutes. The absorbance was taken at 595 nm.

$$\text{Immobilization efficiency} = \frac{(A1 - A2)}{A1} * 100$$

A1: Absorbance of the protein at 595 nm used for immobilization

A2: Absorbance of the protein at 595 nm present in the supernatant

4.7.2 Enzyme Activity

E. coli asparaginase exhibits similar activity against its natural substrate, L-asparagine, and synthetic substrate hydroxamate (AHA). The assay is based on the reaction of hydroxylamine liberated from AHA with 8-hydroxyquinoline at high pH. The resulting green oxine dye has an absorption coefficient of about $1.75 * 10^4$ per mol per cm at 710 nm, which is detectable with high sensitivity. At first, a standard curve using different dilutions of commercially available L-asparaginase was prepared. Then, after immobilization, the pellet and the protein were diluted 10 times and incubated with 1mM of AHA for 30 mins at 600 r.p.m at 37 °C. After 30 mins, 24.5% TCA, which acts as a stop solution, was added, and the solution was centrifuged at 2500 r.p.m for 5 minutes. 10 μ l of supernatant was then mixed with 40 μ l of autoclaved MiliQ water, and 200 μ l of freshly prepared oxine was added to it. The mixture was then incubated at 95 °C for 2-3 minutes, and after cooling down, absorbance was taken at 710 nm.

The difference between the free enzyme activity before immobilization and the activity of the free enzyme left in the supernatant following immobilization divided by the free enzyme activity before immobilization is known as the immobilization efficiency or IE (%).

$$\text{IE (\%)} = \frac{\text{Free ASNase Activity} \left(\frac{U}{mL} \right) - \text{ASNase Activity of sup} \left(\frac{U}{mL} \right)}{\text{Free ASNase Activity} \left(\frac{U}{mL} \right)} * 100$$

4.8 Biophysical Characterization of immobilized f-MWCNT

4.8.1 Scanning Electron Microscopy (SEM)

Scanning electron microscopy was used to analyze the changes in the shape, size, and surface morphology of MWCNT after acid-functionalization and immobilization of the L-asparaginase enzyme. After immobilization, the pellet was lyophilized and then dispersed in methanol. The mixture was then bath sonicated for 2-3 minutes, and a 10 μ l sample was placed on a clear small glass slide previously cut with a diamond-cutter using the drop-cast method and dried in a vacuum overnight. 10 nm of gold coating of the samples was done using a sputter-coater. The SEM Supra 55 (Carl Zeiss, Germany) was operated at 5-10 kV, and images of the samples were taken and recorded at different magnifications (500X - 50000X).

4.8.2 Transmission Electron Microscopy (TEM)

Transmission electron microscopy was used to examine the morphology and diameter of the immobilized enzyme on the surface of MWCNT. Both free and immobilized samples were sonicated for 3 minutes before the TEM examination. A drop of the sample is used to prepare the TEM samples. 10 μ l of the sample was carefully positioned on a copper grid that had been Formvar/Carbon coated. Next, a 2% uranyl acetate staining solution was carefully poured onto the surface of the sample-carrying grid. The grid was carefully removed after a brief one-minute incubation period, and any extra stain was eliminated by lightly brushing the edge with filter paper. Following that, the grid was allowed to air dry at ambient temperature. A transmission electron microscope (JEOL-2100F) was operated at 200 kV acceleration voltage, and images were taken at different magnifications (500X-100000X).

4.8.3 Thermogravimetric analysis (TGA)

Thermogravimetric (TG) analysis studies were performed on a Mettler Toledo TGA/DSC 1 STARE system. For each analysis, samples with approximately 5 mg of sample were loaded on an alumina crucible and heated at 10 °C min⁻¹ from 50 °C to 800 °C under airflow while the weight was measured and recorded continuously.

4.8.4 Fourier Transform Infrared Spectroscopy (FT-IR)

FT-IR (Fourier transform infrared spectroscopy) analysis was used to establish immobilization and ascertain the properties of immobilized L-asparaginase samples. Using a BRUKER TENSOR 27 FT-IR, Infrared spectra of the samples were captured at room temperature within the 4500–500 cm⁻¹ range.

4.8.5 Raman spectroscopy

Raman spectra were recorded in a Bruker RFS100/S FT-Raman spectrometer (Nd: YAG laser, 1064 nm excitation) at a power of 200 mV, with 3000 scans at a resolution of 4 cm⁻¹

4.9 Biochemical Characterization of immobilized f-MWCNT

4.9.1 Enzyme kinetics

For the enzyme kinetics study of free and immobilized enzymes, different concentrations of substrates (AHA) are used. The free and immobilized enzymes were incubated for 30 minutes at 37 °C and 62 °C with these different concentrations of AHA. The reaction was then stopped using 24.5% TCA. Oxine dye was used to measure the activity of free and immobilized enzymes, and the absorbance was recorded at 705 nm. The velocity of reactions was calculated using the following formula:

$$\text{Velocity} = \frac{\text{OD difference}}{\text{Absorption coefficient of green oxindole dye} * \text{time}}$$

The Molar absorption coefficient of green oxindole dye is $1.75 \times 10^4 \text{ M}^{-1} \text{ cm}^{-1}$. $1/V$ and $1/[S]$ were calculated and used for plotting the Lineweaver-Burk Plot. V_{max} , K_m , and $\%K_{\text{cat}}$ were calculated for free and immobilized enzymes using the graph.

4.9.2 pH stability

The effect of pH on the relative recovery of activity (RRA) of f-MWCNT was observed using 50 mM Phosphate buffer of different pH ranges from 5.8 to 8 during the immobilization process. The relative recovery of activity was calculated using the following formula:

$$RRA(\%) = \frac{\text{Immobilized } L - \text{asp activity}}{\text{Maximum } L - \text{asp activity}} * 100$$

4.9.3 Stability in PBS and serum stability

The stability of the free enzyme and immobilized enzyme were checked in 1X PBS (pH = 7) and human serum. For serum stability, first, human blood is collected and kept at room temperature for 10-15 minutes. After the blood was clotted, it was centrifuged at 1000-2000 r.p.m for 10-15 minutes, and finally, the serum was collected from the supernatant. Free enzyme and immobilized enzymes were placed in 1x PBS and human serum at 37°C in stirring condition, and each day enzyme activity was measured using AHA as a substrate for 10 days. 24.5% TCA was used to stop the reaction, and oxine dye was used to measure the activity. The absorbance was recorded at 705 nm. The percentage stability was calculated using the following formula:

$$\text{Stability } (\%) = \frac{OD \text{ after incubation}}{OD \text{ before incubation}} * 100$$

4.10 Protease degradation

For the protease degradation study, 4 μg of free and immobilized enzymes were incubated with or without 0.4 μg of recombinant human Asparaginyl Endopeptidase (AEP) (Rand D Systems) and 0.4 μg of recombinant human Cathepsin B (CTSB) for 24 hours. Colorimetric

activity assay was performed with the samples using the synthetic substrate AHA.

4.11 *In-vitro* antigenicity

In-vitro antigenicity study of free and immobilized enzymes was performed using enzyme-linked immunosorbent assay (ELISA). 100 μ l of free and immobilized enzyme with 0.5, 2.5, and 5 μ g/ml concentration was used for coating and incubated overnight for efficient coating. 1% BSA was used for blocking and incubated for 8 hours at room temperature. 1X Phosphate buffered saline and 0.1% Tween 20 detergent (PBST) was used as washing buffer. The primary antibody of L-asparaginase was added to each well and incubated overnight. After washing with PBST, a secondary antibody was added and incubated for 2 hours at room temperature. Washing was performed using PBST to remove excess antibodies. After adding the substrate, i.e., 3,3',5,5'-Tetramethylbenzidine (TMB), the mixture was incubated in the dark. Sulfuric acid was used to terminate the reaction, and absorbance was measured at 450 nm.

4.12 Cell Viability Study

Mitochondrial function and cell viability were measured by the MTT assay. The human cervical cancer cell line HeLa was purchased from NCCS, Pune. The cell lines were grown and maintained using a DMEM medium supplemented with 10% fetal bovine serum. Cells were seeded at 5000 cells/well in a 96-well plate. For each nanomaterial (MWCNT and immobilized f-MWCNT), a stock solution of 1mg/mL particle in culture medium without any additive was prepared, vortexed at maximum speed for 1 min, and bath-sonicated for 5 min. Different concentrations of nanoparticles in culture medium were prepared and used (20–80 μ g/mL). Particle suspension (in phosphate buffer saline (PBS)/0.1% Tween 80) or medium alone was added to each well. Cells were exposed for 24 h to medium alone or in the presence of nanomaterials. At that time, an MTT assay was performed to evaluate the toxicity of nanoparticles on different cell types. After 24h of

treatment with different concentrations of nanoparticles, the cells were incubated with MTT (0.5 mg/ ml) for 4 hours. Then, 100 μ l of MTT Dissolving solution was added into each well to dissolve formazan crystals, the metabolite of MTT. Absorbance was taken at 570 nm.

Also, free and immobilized enzymes with a range of activity were incubated with a HeLa cell line, and an MTT assay was performed to determine the IC₅₀ of free and immobilized enzymes.

Also, Cell counting kit -8 (CCK-8) was purchased from Sigma-Aldrich. CCK-8 enables convenient tests with the help of WST-8 (2-(2-methoxy-4-nitrophenyl)-3-(4-nitrophenyl)-5-(2,4-disulfophenyl)-2H-tetrazolium, monosodium salt), which forms a water-soluble formazan dye following bioreduction in the presence of an electron carrier, 1-Methoxy PMS. 5000 cells per well were first seeded in a 96-well plate and incubated for 24 hours at 37°C and 5% CO₂. Then, 10 μ l of free and immobilized enzymes with different activity ranges were added to the wells. After incubation, 10 μ l of CCK-8 was added to each well and incubated for 1-4 hours. OD was taken at 450 nm.

CHAPTER 5

RESULTS AND DISCUSSION

5.1 Plasmid isolation and restriction digestion of wild-type L-asparaginase and Mutant C:

Plasmid isolation was performed from Wild type-pET28a-DH5 α and Mutant C-pET28a-DH5 α cells by QIAGEN miniprep plasmid isolation kit. The spectrophotometric analysis confirmed that isolated plasmid DNA is highly pure and of satisfactory concentration. Agarose gel electrophoresis (0.8%) was also performed, and bands were observed. For further confirmation, restriction digestion was performed with the respective plasmids, which released the insert size at 1.5kb, corresponding to L-asparaginase size, showing the confirmation of cloning.

Table 5.1: Spectrophotometric analysis of isolated plasmid DNA

S. No	Plasmid	A _{260/280}	Concentration (ng/ μ l)
1.	Wildtype-pET28a-DH5 α	1.9	96.9
2.	MutC-pET28a-DH5 α	1.85	99.6

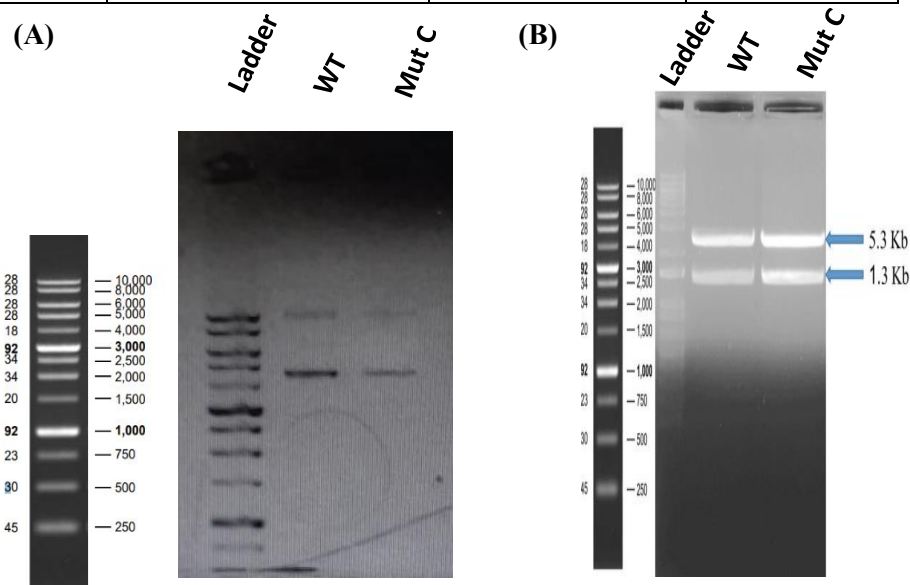


Fig 5.1: (A) 0.8% Agarose gel image of isolated wild-type and Mut C Plasmid, (B) 0.8% Agarose gel image of restriction digested plasmid

5.2 Transformation of wild-type and Mutant C plasmids in *E. coli* BL21(DE3) Cells

Wild-type and Mut C plasmids were transformed in *E. coli* BL21 (DE3) cells by heat shock method, and transformed cells were spread on kanamycin and tetracycline containing LB Agar plates and incubated overnight at 37 °C. Single isolated colonies were observed on the LB Plates, which were further checked by protein isolation and Gram-staining. Three isolated colonies were used to inoculate LB Media, and proteins were isolated. The colonies with maximum protein expression were used for streaking (wild-type colony three and Mut C colony one were selected). Gram-staining results also confirmed that *E. coli*, a rod-shaped, gram-negative bacteria, was successfully isolated.

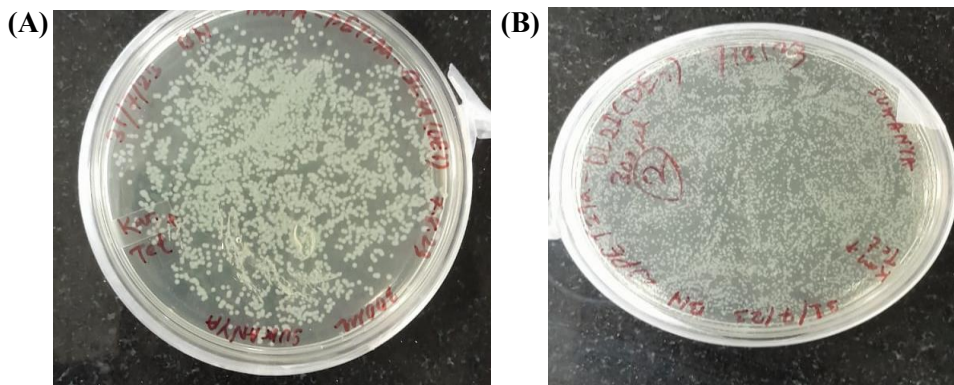


Fig 5.2: (A) Transformed colonies of Mut C-pET28a-BL21(DE3), (B) Transformed colonies of Wildtype-pET28a-BL21(DE3)

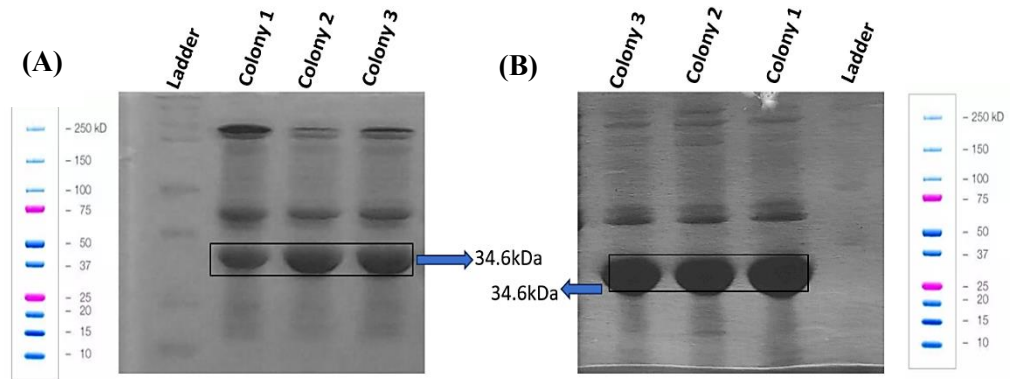


Fig 5.3: (A) 12% SDS-PAGE of isolated protein from transformed colonies of WT-pET28a-BL21(DE3), (B) 12% SDS-PAGE of isolated protein from transformed colonies of Mut C-pET28a-BL21(DE3)

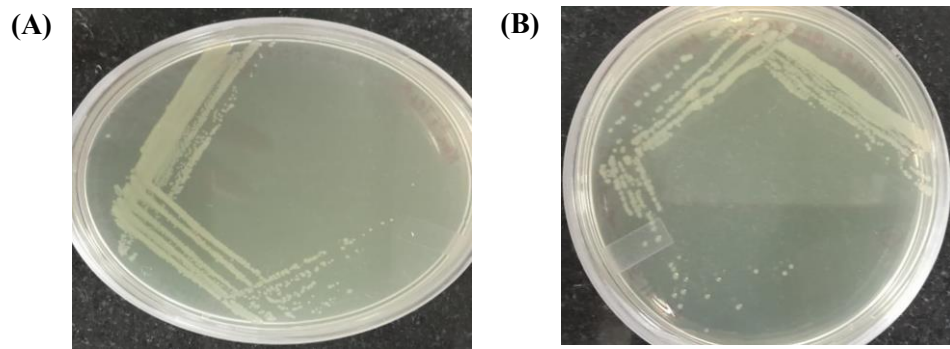


Fig 5.4: (A) Streaked plate of WT-pET28a-BL21(DE3) from colony 3, (B) Streaked plate of Mut C-pET28a-BL21(DE3) from colony 1

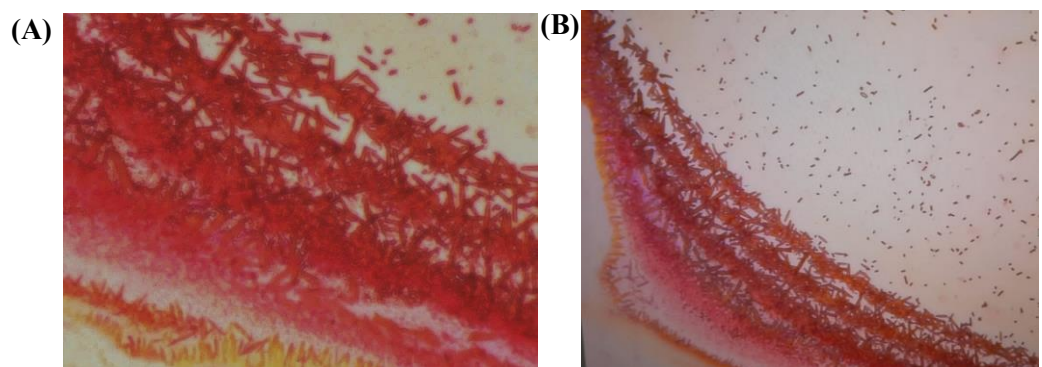


Fig 5.5: (A) 100x microscopic image after Gram-staining of WT-pET28a-BL21(DE3), (B) 100x microscopic image after Gram-staining of Mut C-pET28a-BL21(DE3)

5.3 Isolation of recombinant L-asparaginase

Wild-type and Mut C L-asparaginase were isolated using the osmotic shock method by a hypertonic solution. 0.5 mM IPTG (Isopropyl 1- β -D thiogalactopyranoside) was used to induce the bacterial culture for 1,2,3,4,5 and 6 hours, and 12% SDS-PAGE was performed to check the protein expression. Maximum expression of wild type and Mut C was observed after 4 hours of IPTG induction.

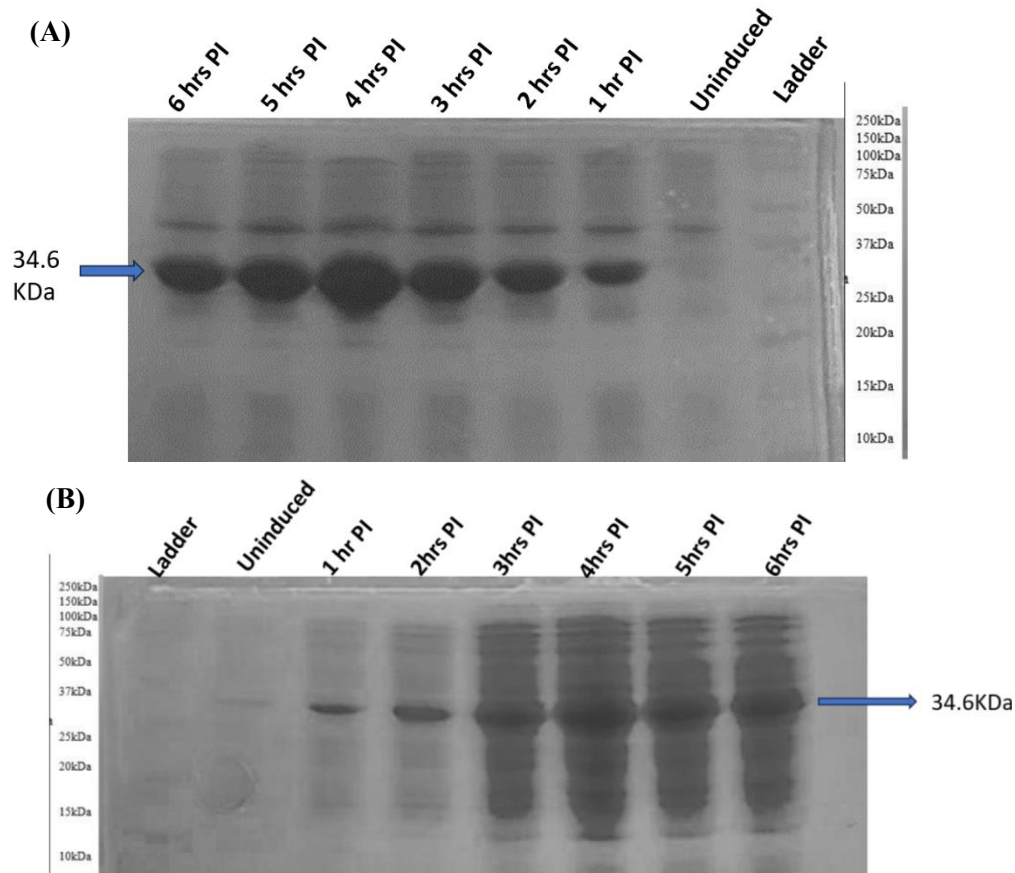


Fig 5.6: (A) 12% SDS-PAGE image of wild-type crude protein after 1,2,3,4,5,6 hours of IPTG induction, (B) 12% SDS-PAGE image of Mut C crude protein after 1,2,3,4,5,6 hours of IPTG induction, PI: Post induction

5.4 Purification of Wild-type and Mut C L-asparaginase

The crude protein, isolated from a single transformed colony, was contaminated with other periplasmic proteins. Contamination of L-asparaginase with glutaminase or urease can show side effects in the human body. Therefore, high purity of clinical L-asparaginase is required before administration in humans. Further purification was achieved by a multi-step purification process which includes gradient ammonium sulphate precipitation (50% and 90%), dialysis, anion-exchange, and size-exclusion chromatography using AKTA purification system 12% SDS-PAGE was performed to check the purity of protein after the multi-step purification. A decreasing number of other protein bands was observed during each purification step. In anion-exchange and size-exclusion chromatography, a sharp peak of protein at 280nm was observed, depicting the purity of the enzyme.

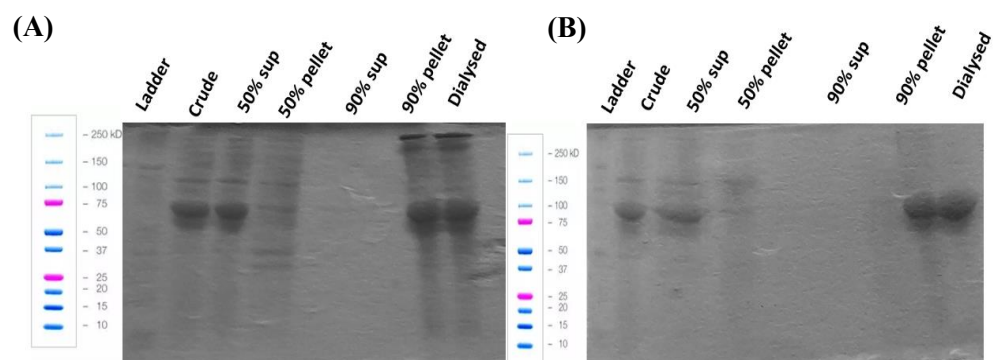


Fig 5.7: (A) Wild-type L-asp purification by ammonium sulphate precipitation and dialysis,(B) Mut C L-asp purification by ammonium sulphate precipitation and dialysis

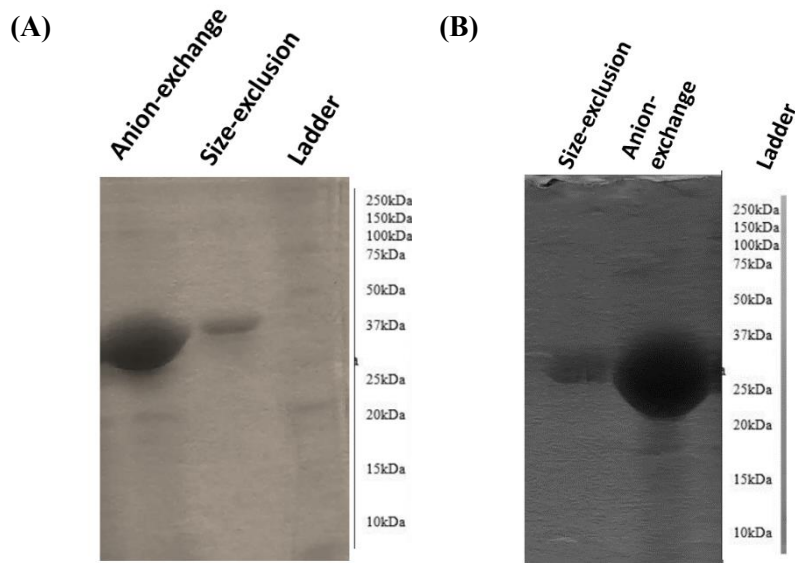
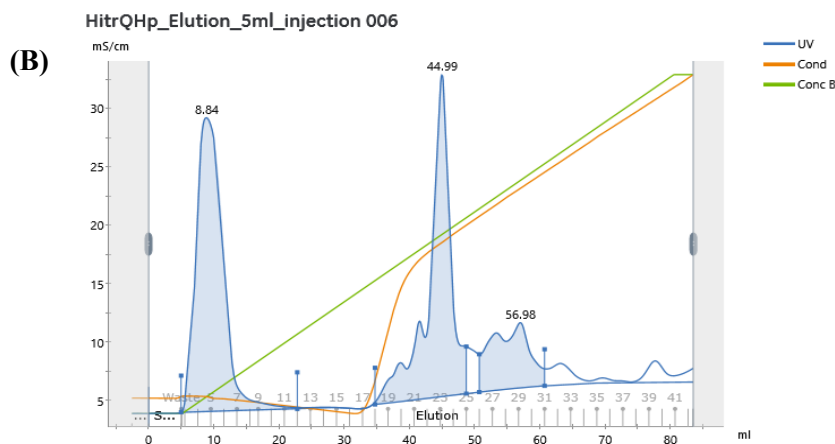
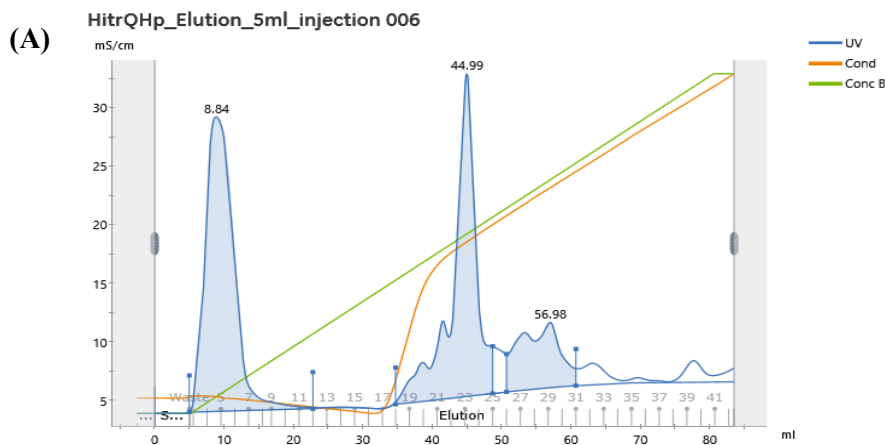


Fig 5.8: (A) Wild-type L-asp purification by anion-exchange and size-exclusion chromatography, (B) Mut C L-asp purification by anion-exchange and size-exclusion chromatography



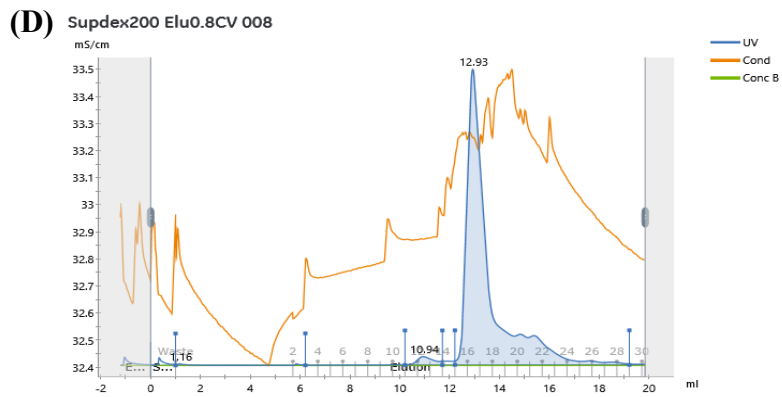
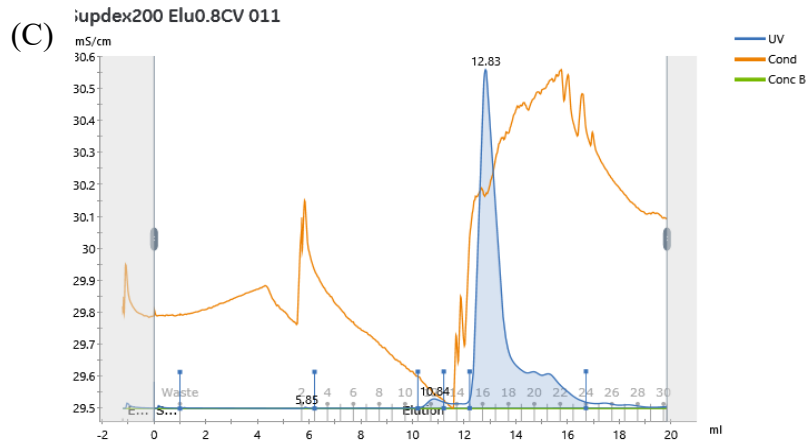
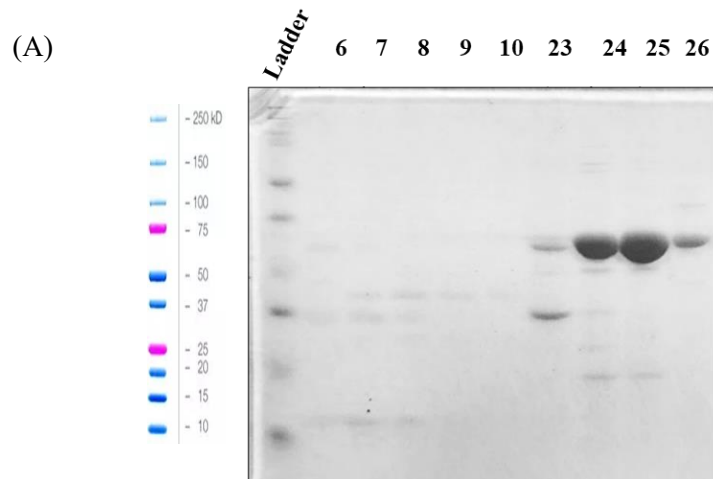


Fig 5.9: (A) Chromatogram of purified Wild-type L-asparaginase protein by anion-exchange chromatography,(B) Chromatogram of purified Mut C L-asparaginase protein by anion-exchange chromatography,(C) Chromatogram of purified Wild-type L-asparaginase protein by size-exclusion chromatography,(D) Chromatogram of purified Mut C L-asparaginase protein by size-exclusion chromatography



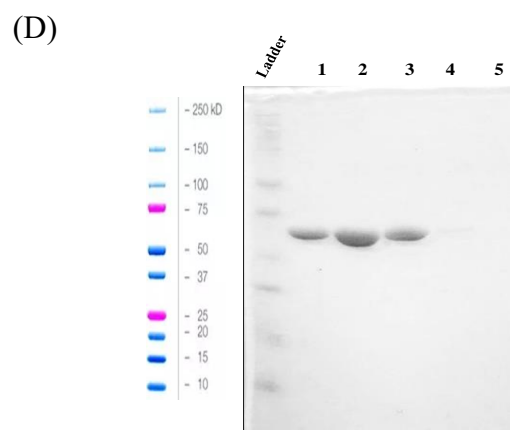
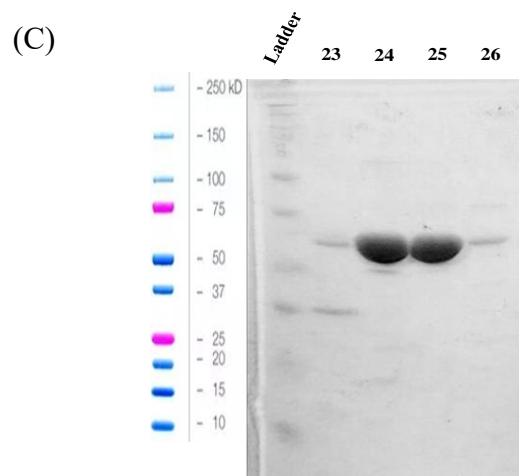
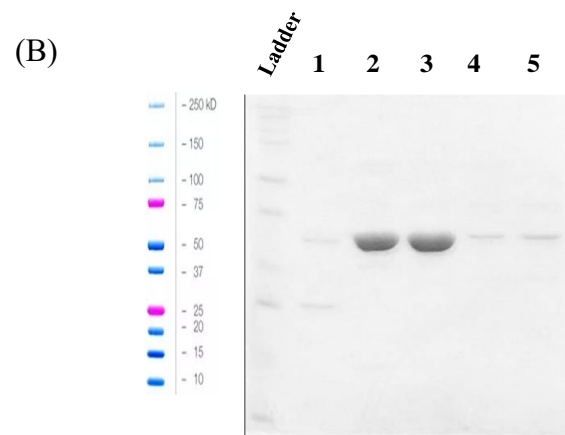


Fig 5.10: 12% SDS-PAGE of Mut C L-asparaginase after purification by (A) anion-exchange and (B) size-exclusion chromatography, 12% SDS-PAGE of wild-type L-asparaginase after purification by (C) anion-exchange and (D) size-exclusion chromatography

5.5 Concentration determination of protein using the Bradford method

The concentrations of concentrated wild-type and Mutant C proteins were determined using the Bradford method. At first, a Bovine serum albumin (BSA) standard curve was made using different dilutions of 10 mg/ml BSA stock. Protein concentration was determined using the equation shown in the graph.

Table 5.2: Concentrations of pure-proteins

Protein	Conc (mg/ml)
Wild-type	0.55
Mut C	1.8

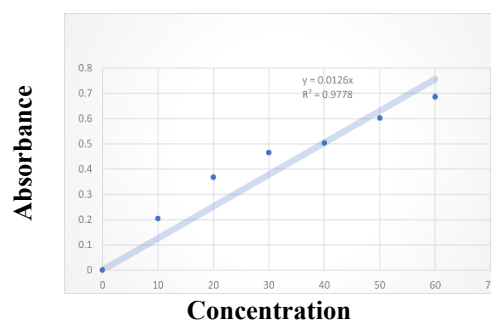


Fig 5.11: BSA Standard curve

5.6 Immobilization of L-asparaginase on copolymers

Immobilization efficiency of PMMA, copolymers of MMA and AA, and MMA and GMA were calculated using Bradford method and absorbance was taken at 595nm. The following formula was used to calculate immobilization efficiency:

$$\text{Immobilization efficiency} = \frac{(A1 - A2)}{A1} * 100$$

A1: Absorbance of the protein at 595 nm used for immobilization

A2: Absorbance of the protein at 595 nm present in the supernatant

PMMA showed no immobilization, the copolymer of MMA and AA showed around 42.84% and the copolymer of MMA and GMA (7:3) showed an immobilization yield of 43.7%, and a copolymer of MMA and GMA(3:7) showed immobilization yield of 49.31% initially, but when we checked the wash for the presence of protein, we got much amount of protein concentration present in the supernatant. Therefore,

we can conclude protein is not immobilized in sufficient amounts on the surface of polymers and copolymers.

5.7 Immobilization of L-asparaginase on f-MWCNT

Immobilization of L-asparaginase on the surface of functionalized MWCNT was determined using the Bradford method and enzyme activity assay. It has been observed that with increasing concentration of L-asparaginase, immobilization yield is increasing, and the highest yield of $95.87 \pm 4.8\%$ was observed at a concentration of 1.5 mg/ml L-asparaginase.

Table 5.3: Immobilization efficiency (IE) at different concentrations of L-asparaginase

Concentration of protein (mg/ml)	IE (%)
0.25	63.29 ± 13.33
0.5	73.24 ± 11.34
0.75	93.90 ± 5.42
1	95.6 ± 0.54
1.25	95.8 ± 6.5
1.5	95.87 ± 4.8

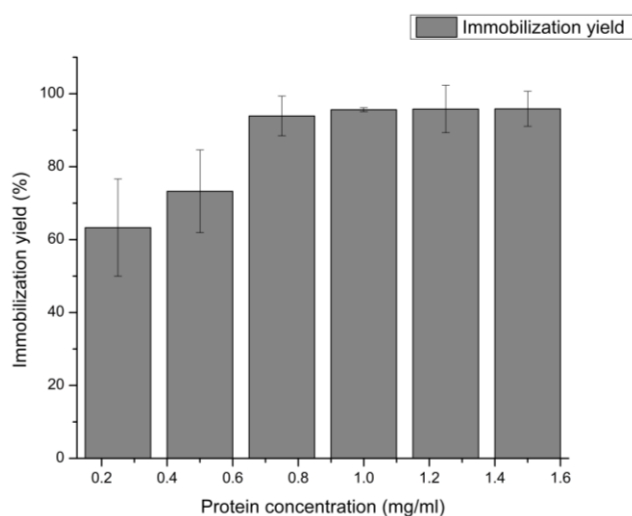


Fig 5.12: Effect of L-asparaginase concentration on immobilization yield

We have also determined Immobilization yield using enzyme activity assay. The highest immobilization yield was $95.95\% \pm 0.08$ at a concentration of 1mg/ml L-Asparaginase.

Table 5.4: Immobilization efficiency (IE) at different concentrations of L asparaginase

Concentration of protein(mg/ml)	IE (%)
0.25	93.73 ± 1.62
0.5	93.89 ± 2.26
0.75	91.59 ± 7.37
1	95.95 ± 0.08
1.25	95.81 ± 5.29
1.5	95.81 ± 0.98

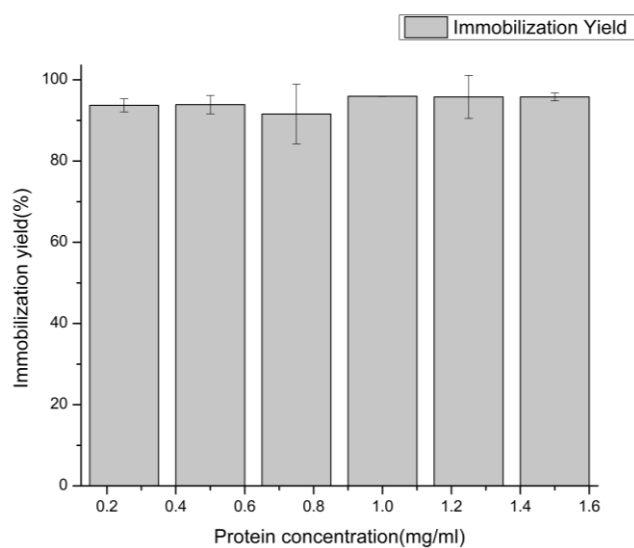


Fig 5.13: Effect of L-asparaginase concentration on immobilization yield

5.8 Biophysical Characterization of immobilized f-MWCNT

5.8.1 Scanning electron microscopy (SEM)

Changes in the surface morphology of bare MWCNTs, acid-functionalized MWCNT, and immobilized L-asparaginase preparations were characterized by SEM analysis. As shown in Fig. 5.13, a typical tubular morphology of MWCNT was observed; acid-functionalized MWCNT contains more open ends because acid treatment caused breaks in the MWCNT walls, and the surface morphology of L-asparaginase immobilized f-MWCNT preparations was much rougher and thicker than that of the bare MWCNTs as a result of modification and immobilization. Similar findings have been reported for different enzymes immobilized on MWCNTs.

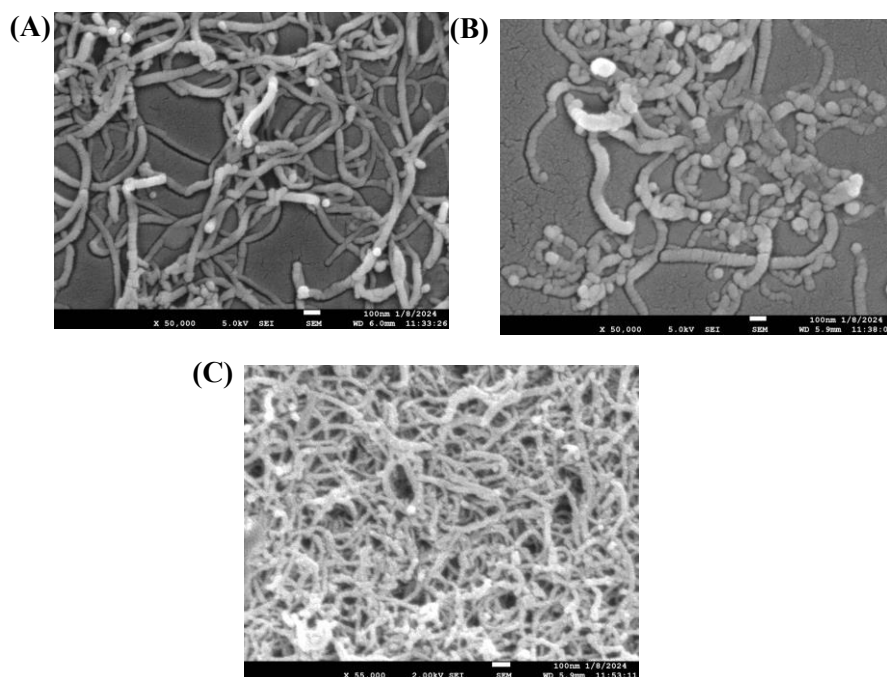


Fig 5.14: (A) SEM image of MWCNT, (B) SEM image of f-MWCNT, (C) SEM image of immobilized f-MWCNT

5.8.2 Transmission electron microscopy (TEM)

The immobilization of $1.5 \times 10^{-3} \text{ mg mL}^{-1}$ of L-asp over the MWCNTs was also confirmed by TEM, as displayed in Fig. 5.14 for MWCNT and

L-Asp immobilized f-MWCNT. Typical tubular morphology of MWCNTs was observed, as well as the opened ends of the tubes (Fig.5.14. A). After L-asparaginase immobilization, the walls of the MWCNTs become thicker and more irregular due to the presence of the enzyme at the surface of the MWCNT (Fig. 5.14.B). The difference between the thickness of the untreated MWCNT and the L-asparaginase-immobilized f-MWCNT nano-bioconjugate gives an estimated thickness of the enzyme film of 9 nm.

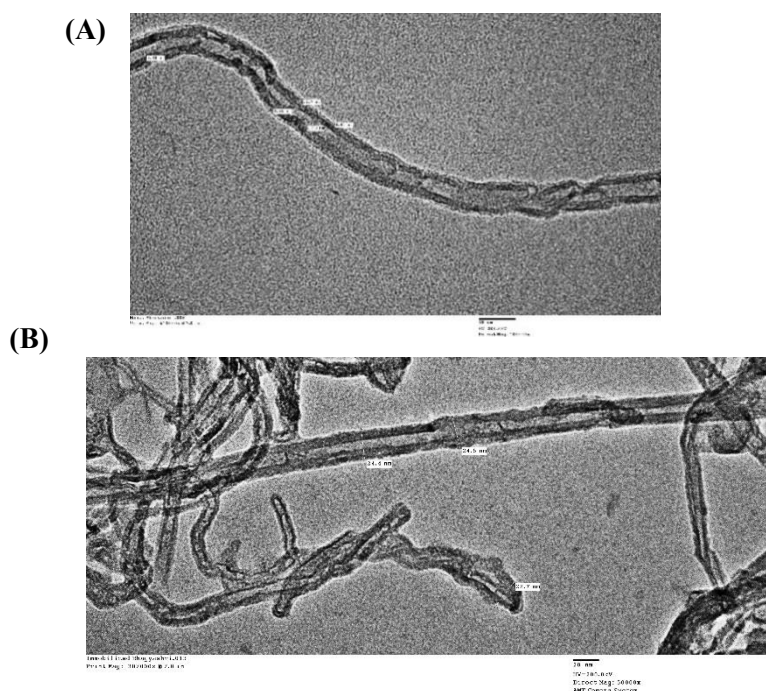


Fig 5.15: (A)TEM image of untreated MWCNT, (B) TEM image of immobilized f-MWCNT

5.8.3 Thermogravimetric analysis (TGA)

Thermogravimetric analysis (TGA) of untreated MWCNT and the respective L-asparaginase bioconjugate, L-asparaginase-f-MWCNT (immobilization with 1.5×10^{-3} mg mL⁻¹ of L-asparaginase per 2 mg of material), is presented in Fig. 5.15. TGA results it has been observed that the MWCNT starts to decompose at around 580 °C. In the case of L-asparaginase immobilized f-MWCNT, two main weight losses are observed. The first weight loss is detected at around 250 °C, which is attributed to the thermal decomposition of the enzyme, while the

second weight loss at 600 °C is recognized as the simultaneous pyrolysis of L-asparaginase and MWCNTs, attaining a plateau at a temperature near to 700 °C.

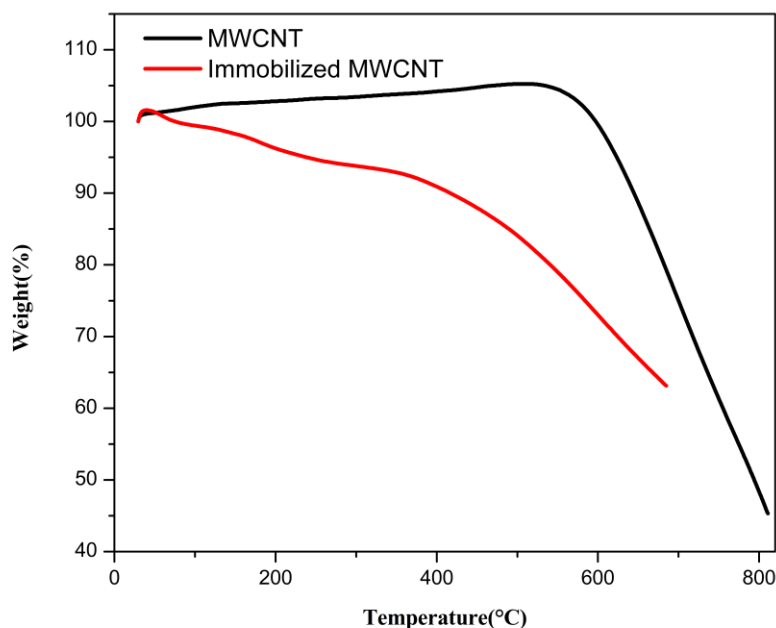


Fig 5.16: TGA Analysis of MWCNT-Before and after immobilization

5.8.4 Fourier Transform Infrared Spectroscopy (FT-IR)

FT-IR spectra of untreated MWCNT, acid-functionalized MWCNT, and its immobilized counterparts in the range 4000–450 cm^{-1} are shown in Fig. 5.16. In the case of the MWCNT spectrum, the asymmetric methyl stretching band at 2960 cm^{-1} and asymmetric/symmetric methylene stretching bands at 2923 and 2853 cm^{-1} are observed, respectively. It is usually assumed that these groups are located at the defect sites on the sidewall surface. The bands at 1539 cm^{-1} and 2115 cm^{-1} are due to stretching of C=C and C=C stretching respectively.

In the case of MWCNT-COOH, the presence of these additional bands at 1560 cm^{-1} , 1717 cm^{-1} , and 1732 cm^{-1} are observed that corresponds to carboxylate anion stretch mode and C=O vibration, respectively. The

broad band at 3320 cm^{-1} and 3436 cm^{-1} are due to the stretching vibration of the OH group.

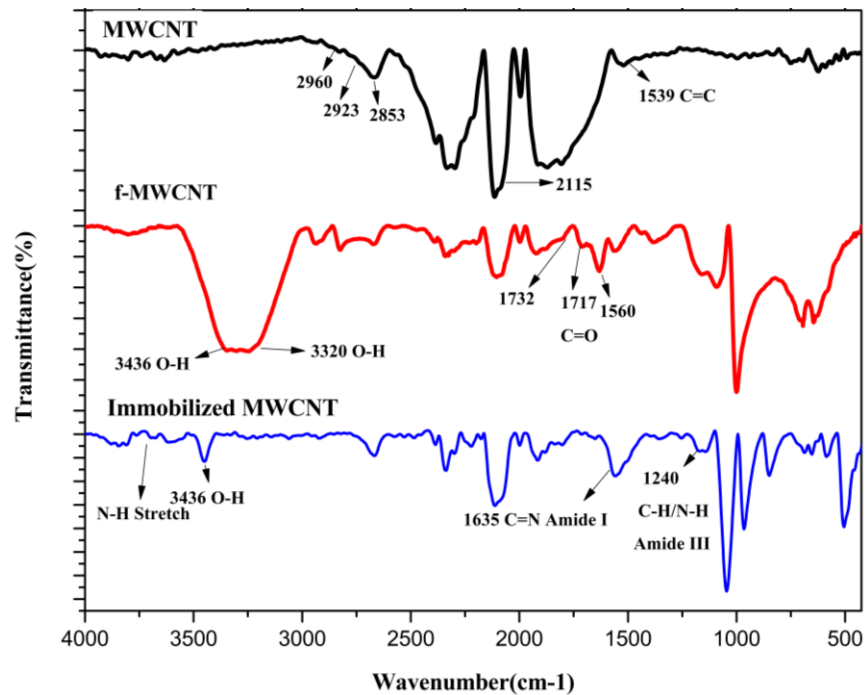


Fig 5.17: FT-IR Spectra of MWCNT- Before and after immobilization

In the case of immobilized f-MWCNT, the broadband in the range $3600\text{--}4000\text{ cm}^{-1}$ shows the N–H stretch of the -NH_2 group. The peak at 1635 cm^{-1} refers to the amide bond of the enzyme. The vibrations in the $1200\text{--}800\text{ cm}^{-1}$ range correspond to C–N, C–O, and C–C stretching in the enzyme molecule. The characteristic peaks observed at 1240 and 3629 cm^{-1} in the structure of the immobilized enzymes correspond to the amide III bond and -NH_2 group, respectively. The presence of these peaks confirmed the immobilization of L-asparaginase.

5.8.5 Raman spectroscopy

Raman spectroscopy was also used for the characterization of functionalized MWCNT and immobilized MWCNT. Two characteristic bands, i.e., “G” and “D” bands at 1600 cm^{-1} and 1287 cm^{-1} , respectively, were observed in the range of $1000\text{--}2000\text{ cm}^{-1}$. The G band is associated with the regular sp^2 graphitic network of MWCNT is shared by both materials, and the D band is attributed to the disorder and flaws in the lattice that result from sp^3 hybridized carbon.

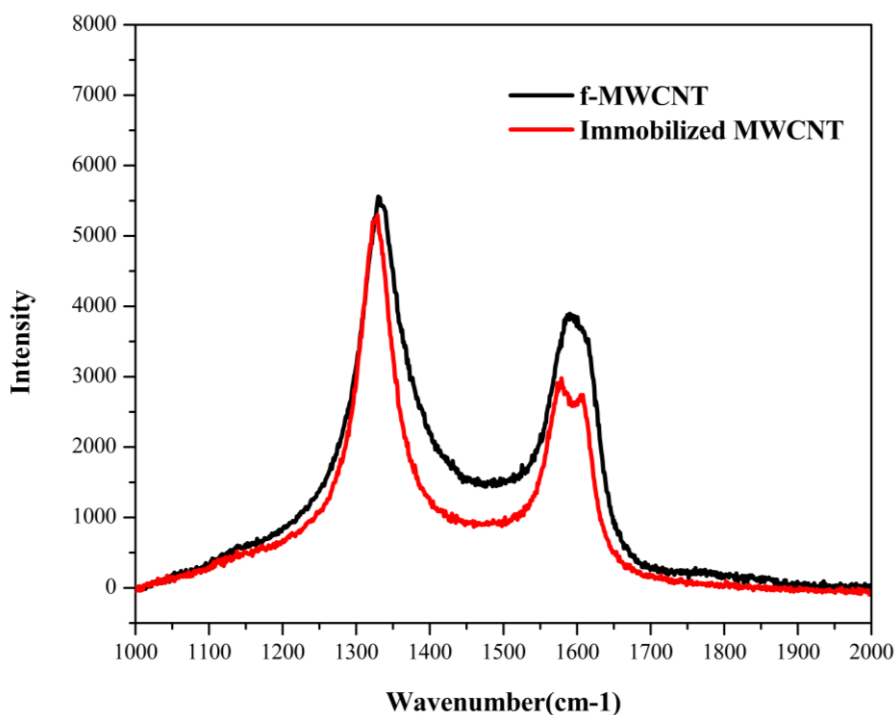


Fig 5.18: Raman spectra of MWCNT and immobilized MWCNT

The degree of disorder and the presence of defect sites in the MWCNTs lattice is determined by the ratio (I_D/I_G) between the intensities of the D and G bands. The I_D/I_G values obtained for MWCNT and Immobilized MWCNT were 1.4 and 1.5, respectively. These similar values suggest that the enzyme immobilization in the nanomaterials does not cause a significant disturbance on the CNTs surface, indicating similar degrees of disorder, i.e. the majority of L-asparaginase adsorption happens on the surface defects of f-MWCNT, which does not alter the sp^2 and the concentration of sp^3 bonds.

5.9 Biochemical characterization of immobilized f-MWCNT

5.9.1 Enzyme kinetics

The kinetic parameters are essential for the prediction of the activity of free and immobilized enzymes. Here, the enzyme kinetics study was performed using different concentrations of synthetic substrate AHA at physiological temperatures (37 °C) and 62 °C. Velocity vs substrate concentrations graphs are plotted for both free and immobilized enzymes. $1/V$ and $1/[S]$ were used to plot the Lineweaver Burk Plot

from which the values of K_m , V_{max} , and K_{cat} were obtained. % K_{cat} was also obtained and plotted for free and immobilized enzymes at 37 °C and 62 °C.

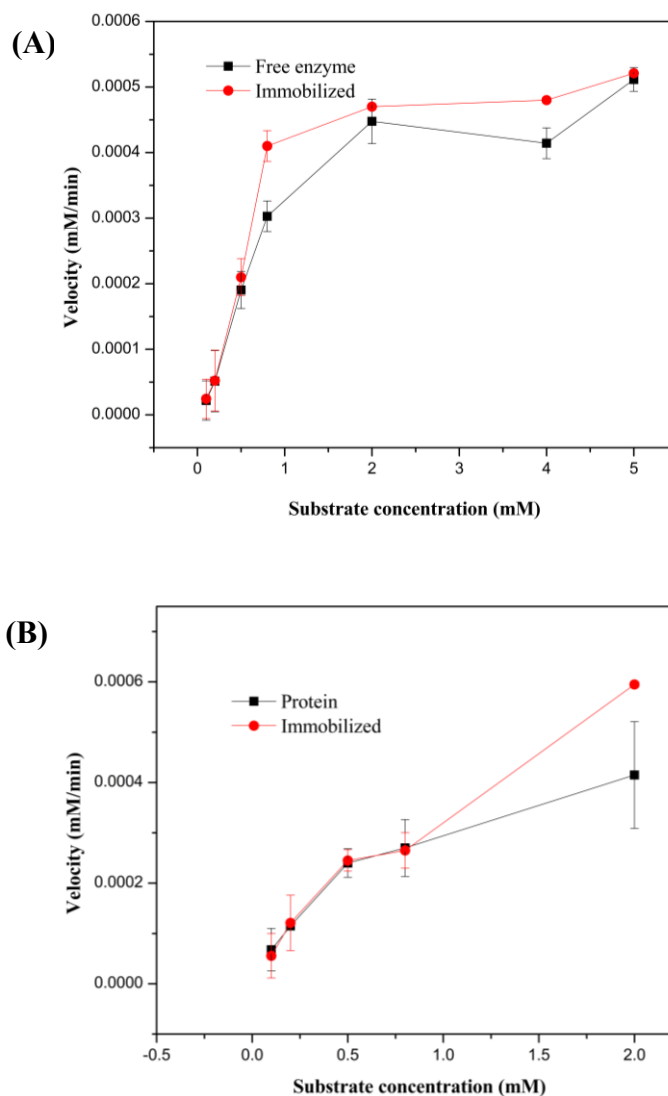


Fig 5.19: (A) Velocity vs substrate concentration plot for free and immobilized enzymes at 37 °C, (B) Velocity vs substrate concentration plot for free and immobilized enzymes at 62 °C

Table 5.5: The kinetic parameters for each enzyme at 37 °C

Enzymes	Km (mM)	Vmax (mM/sec)	Kcat	Kcat%
Mut-C	0.467	0.000045	0.000096	100
Immobilized	0.456	0.000047	0.0001	107.36

Table 5.6: The kinetic parameters for each enzyme at 62 °C

Enzymes	Km (mM)	Vmax (mM/sec)	Kcat	Kcat%
Mut-C	0.5467	0.000057	0.001	100
Immobilized	0.8817	0.000084	0.00095	95.35

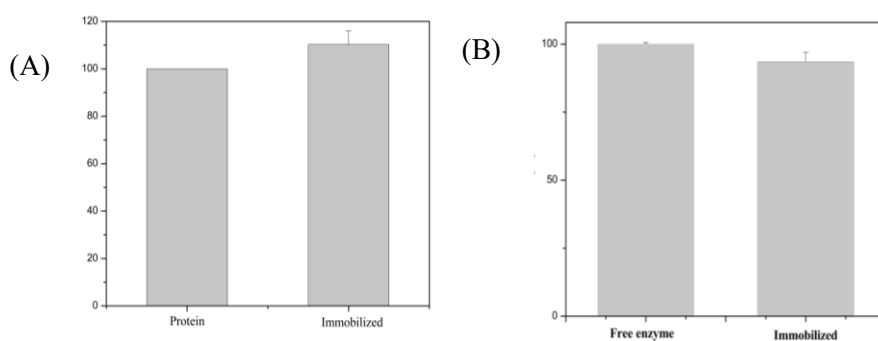


Fig 5.20: (A) Kcat % of the free and immobilized enzyme at 37 °C,

(B) Kcat % of the free and immobilized enzyme at 62 °C

5.9.2 pH stability

For the pH stability study, free and immobilized enzymes were incubated at different pH ranges (5.8 to 8) and then enzyme activity was checked. **Fig. 5.21** shows that the immobilized enzyme has a better stability profile in comparison to the free enzyme. Both free and immobilized enzymes showed the highest stability at pH 7.

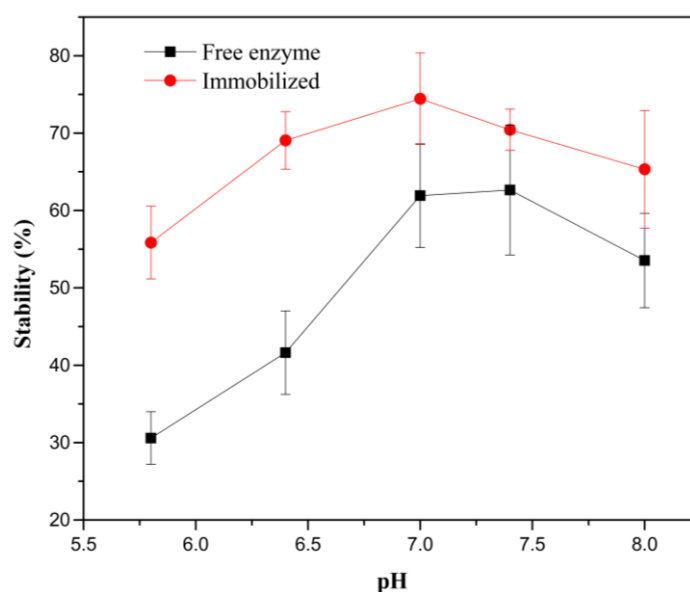


Fig 5.21: pH stability of free and immobilized enzymes

5.9.3 PBS and serum stability

For the PBS stability study, free and immobilized enzymes were incubated at stirring conditions at 37 °C for 10 days. Each day enzyme activity was checked using AHA as a synthetic substrate. Fig 5.22 (A) shows that immobilized enzyme is more stable in 1x PBS (pH = 7.2). For serum stability study, blood is centrifuged at 1000-2000 r.p.m for 10-15 minutes. Then, serum was isolated, and free and immobilized enzymes were incubated in serum at stirring conditions at 37 °C for 10 days. Each day enzyme activity was checked using AHA as a synthetic substrate. Fig 5.22 (B) shows that immobilized enzyme is more stable in 1x PBS human serum in comparison to free enzyme.

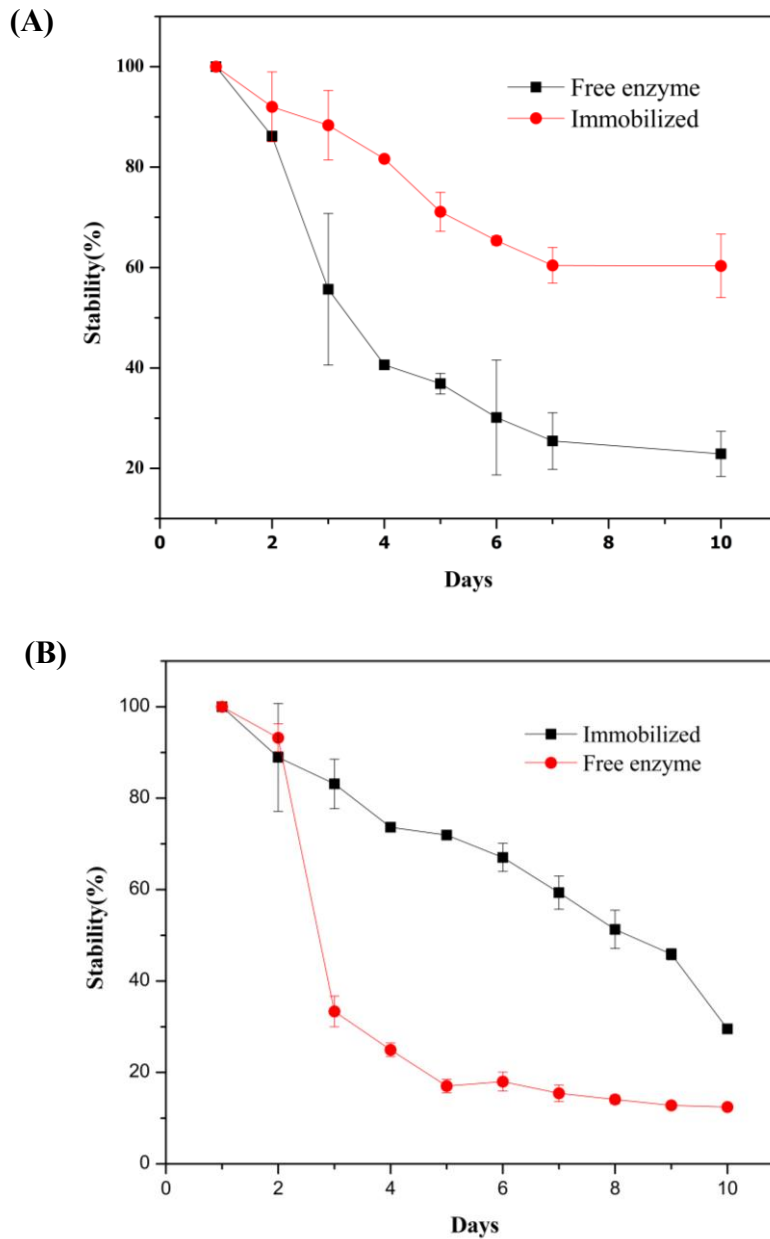


Fig 5.22: (A) PBS Stability profile of the free and immobilized enzyme, (B) Serum Stability profile of the free and immobilized enzyme

5.10 Protease degradation

The Protease degradation study of free and immobilized enzymes was performed using Acetyl endopeptidase (AEP) and Cathepsin B (CTSB). After 24 hours of incubation, the relative activity of the free enzyme was slightly lesser than the free enzyme; therefore, the free

enzyme showed slightly more degradation than the immobilized enzyme.

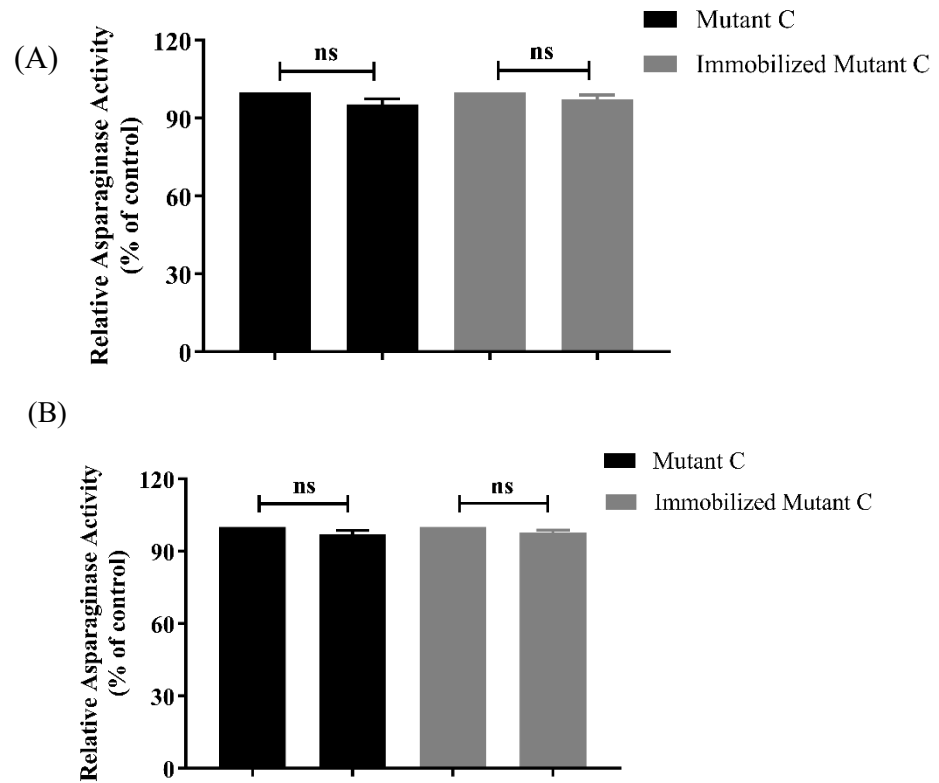


Fig 5.23: (A) Degradation study of Free and Immobilized L-asparaginase using AEP, (B) Degradation study of Free and Immobilized L-asparaginase using CTSSB

5.11 *In-vitro* antigenicity

One of the major drawbacks of the L-asparaginase enzyme is the formation of anti-drug antibodies (ADA), which cause hypersensitivity reactions in most ALL patients, and silent inactivation, which removes L-asparaginase from the circulation rapidly. Here, we checked the binding of the anti-asparaginase antibody to the free enzyme (Mut C) and immobilized enzyme. Immobilized enzyme showed a significant reduction (around 35%) in antibody binding compared to free enzyme. ($P > 0.05$).

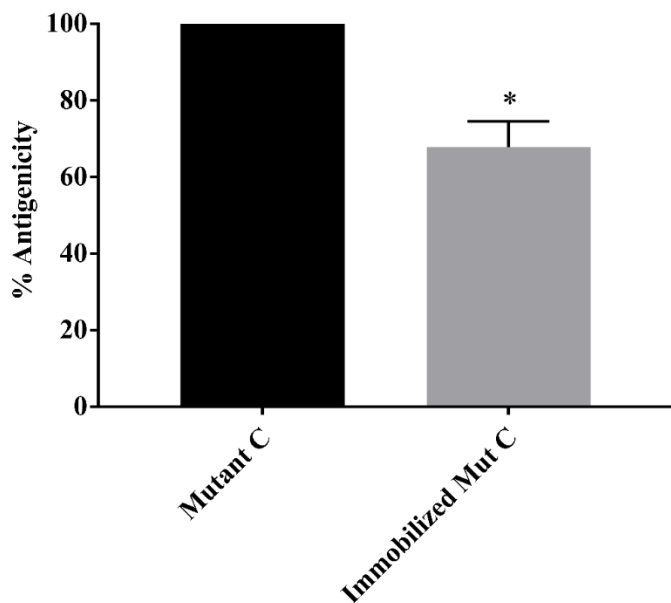
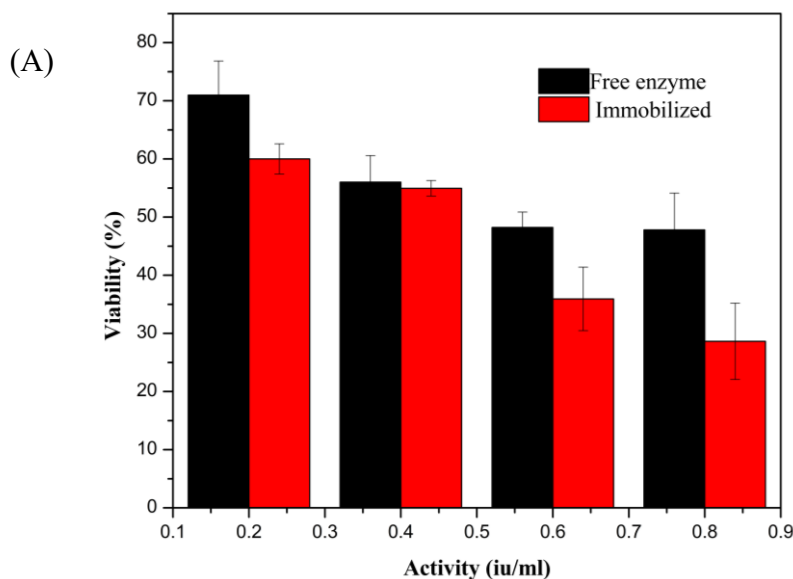


Fig 5.24: The *in-vitro* antigenicity of free v/s immobilized L-asparaginase was determined by indirect ELISA (*significance was analyzed by one-way ANOVA using GraphPad Prism version 7.0 where *p<0.05)

5.12 Cell viability assay

Cell viability of the HeLa cell line was tested after 24 hours of treatment with untreated MWCNT and acid-functionalized MWCNT using MTT assay. In the case of untreated MWCNT, the cell viability decreases with increasing concentration of particles, whereas less decrement in the cell viability was observed in the case of f-MWCNT.



(B)

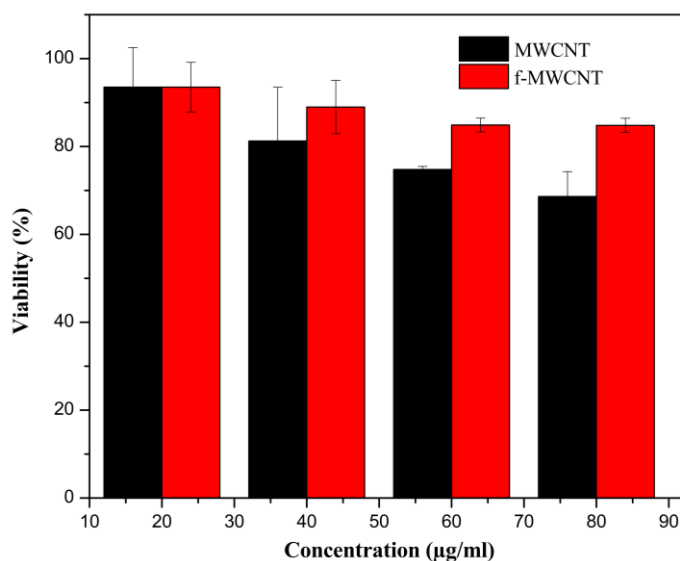


Fig 5.25: (A) Cell viability of HeLa cells cultured with untreated MWCNT and functionalized MWCNT of different concentrations after 24 hours, (B) Cell viability of HeLa cells cultured with free and immobilized enzymes of different activity ranges.

Cell viability assay was also performed using free and immobilized enzymes of different ranges of activity (0, 0.2, 0.4, 0.6, 0.8 IU/ml). The immobilized enzyme is more efficiently killing the HeLa cells than the free enzyme may be due to sustainable release or less degradation of the enzyme. The IC₅₀ values of free and immobilized enzymes were 0.2952 ± 0.1 IU/ml and 0.4092 ± 0.1 IU/ml, respectively.

Cell viability assay was also performed in the MOLT-4 cell line using CCK-8 from Sigma-Aldrich. In the MOLT-4 cell line, similar results were observed that of HeLa. The immobilized enzyme is more efficiently killing the MOLT-4 cells than the free enzyme may be due to sustainable release or less degradation of the enzyme. The IC₅₀ values of free and immobilized enzymes were 0.3271 ± 0.09 IU/ml and 0.4018 ± 0.1 IU/ml, respectively.

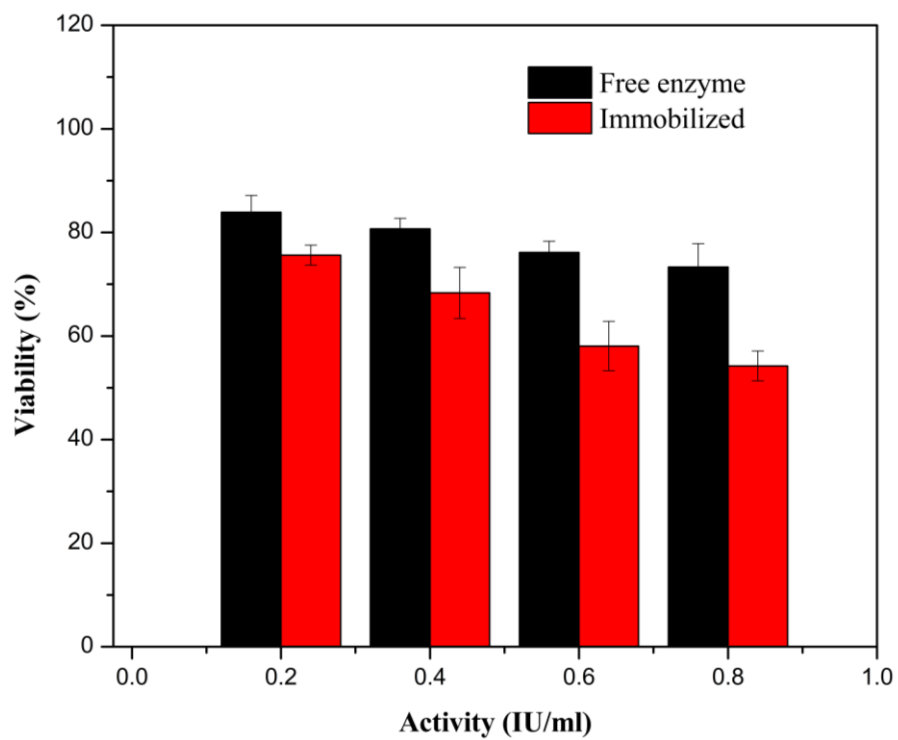


Fig 5.26: Cell viability of MOLT-4 cells cultured with free and immobilized enzymes of different activity ranges

CHAPTER 6

Conclusions and future work

In conclusion, we have wild-type and chemically modified L-asparaginase mutants prepared in our lab. we have successfully isolated and purified the wild-type and Mutant C L-asparaginase and also checked its purity in 12% SDS-PAGE. We have synthesized polymers and copolymers using MMA, AA, and GMA and tried to immobilize L-asparaginase but it does not give any satisfactory results. We have also functionalized the multi-walled carbon nanotube (MWCNT) with carboxyl groups, and it has been activated using EDC and N-hydroxy succinimide (NHS). Immobilization results of L-asparaginase onto the f-MWCNT show the highest immobilization yield of 95.87%. Scanning electron microscopy (SEM), Transmission electron microscopy (TEM), Thermogravimetric analysis (TGA), Fourier Transform Infra-red spectroscopy (FT-IR), and Raman Spectroscopy results also confirm the L-asparaginase immobilization on the f-MWCNT surface. Immobilized enzymes showed better pH stability and stability in PBS and human serum than the free enzymes. Immobilized enzymes also showed better kinetic properties at 37 °C and were stable at both 37 °C and 62 °C. Immobilized enzymes have lower antigenicity and are stable in the presence of proteases like Cathepsin B and Acetyl endopeptidase. Immobilized enzymes also showed greater efficiency in killing the HeLa and MOLT-4 cells than the free enzyme may be due to sustainable release or less degradation of the enzyme. Our findings may contribute to the creation of innovative, chemically altered L-asparaginase medications with fewer adverse effects. The potential for these altered new variant absence of side effects to enhance treatment outcomes generally and might serve as a standard in asparaginase therapy for the management of everyone. Therefore, it may be beneficial to ALL patients.

CHAPTER 7

REFERENCES

1. No Title. <https://seer.cancer.gov/statfacts/html/aly1.html>.
2. Malard, F. & Mohty, M. Acute lymphoblastic leukaemia. *Lancet* **395**, 1146–1162 (2020).
3. Juluri, K. R., Siu, C. & Cassaday, R. D. Asparaginase in the Treatment of Acute Lymphoblastic Leukemia in Adults: Current Evidence and Place in Therapy. *Blood Lymphat. Cancer Targets Ther.* **Volume 12**, 55–79 (2022).
4. Whitlock, J. A. Down syndrome and acute lymphoblastic leukaemia. *Br. J. Haematol.* **135**, 595–602 (2006).
5. No Title.
<https://www.msmanuals.com/professional/hematology>.
6. No Title. <https://www.lls.org/leukemia/acute-lymphoblastic-l>.
7. Ghasemian, A. *et al.* Bacterial l-asparaginases for cancer therapy: Current knowledge and future perspectives. *J. Cell. Physiol.* **234**, 19271–19279 (2019).
8. Tong, W. H. *et al.* A prospective study on drug monitoring of PEGasparaginase and Erwinia asparaginase and asparaginase antibodies in pediatric acute lymphoblastic leukemia. *Blood* **123**, 2026–2033 (2014).
9. Michalska, K. & Jaskolski, M. Structural aspects of L-asparaginases, their friends and relations. *Acta Biochim. Pol.* **53**, 627–640 (2006).
10. Mehta, R. K. *et al.* Mutations in subunit interface and B-cell Epitopes improve Antileukemic activities of Escherichia Coli asparaginase-II: Evaluation of Immunogenicity in Mice. *J. Biol. Chem.* **289**, 3555–3570 (2014).
11. Swain, A. L., Jaskolski, M., Housset, D., Rao, J. K. M. &

- Wlodawer, A. Crystal structure of Escherichia coli L-asparaginase, an enzyme used in cancer therapy. *Proc. Natl. Acad. Sci. U. S. A.* **90**, 1474–1478 (1993).
12. Asselin, B. L. Comparative Pharmacology and Optimal Use in Childhood. *Drug Resist. Leuk. Lymphoma III* 621–629 (1999).
 13. Chan, W. K. *et al.* The glutaminase activity of L- Asparaginase is not required for anticancer activity against ASNS-negative cells. *Blood* **123**, 3596–3606 (2014).
 14. Chan, W. K. *et al.* Glutaminase activity of L-asparaginase contributes to durable preclinical activity against acute lymphoblastic leukemia. *Mol. Cancer Ther.* **18**, 1587–1592 (2019).
 15. Fonseca, M. H. G., Fiúza, T. da S., Morais, S. B. de, Souza, T. de A. C. B. de & Trevizani, R. Circumventing the side effects of L-asparaginase. *Biomed. Pharmacother.* **139**, (2021).
 16. Sengupta, S. *et al.* Preclinical evaluation of engineered L-asparaginase variants to improve the treatment of Acute Lymphoblastic Leukemia. *Transl. Oncol.* **43**, (2024).
 17. Villanueva-Flores, F., Zárate-Romero, A., Torres, A. G. & Huerta-Saquero, A. Encapsulation of asparaginase as a promising strategy to improve in vivo drug performance. *Pharmaceutics* **13**, 1–19 (2021).
 18. Bettencourt, A. & Almeida, A. J. Poly(methyl methacrylate) particulate carriers in drug delivery. *J. Microencapsul.* **29**, 353–367 (2012).
 19. Ulu, A., Koytepe, S. & Ates, B. Design of starch functionalized biodegradable P(MAA-co-MMA) as carrier matrix for L-asparaginase immobilization. *Carbohydr. Polym.* **153**, 559–572 (2016).
 20. Yan, X. & Gemeinhart, R. A. Cisplatin delivery from

- poly(acrylic acid-co-methyl methacrylate) microparticles. *J. Control. Release* **106**, 198–208 (2005).
21. Nita, L. E., Chiriac, A. P. & Nistor, M. An in vitro release study of indomethacin from nanoparticles based on methyl methacrylate/glycidyl methacrylate copolymers. *J. Mater. Sci. Mater. Med.* **21**, 3129–3140 (2010).
 22. Madani, S. Y., Naderi, N., Dissanayake, O., Tan, A. & Seifalian, A. M. A new era of cancer treatment: carbon nanotubes as drug delivery tools. *Int. J. Nanomedicine* **6**, 2963–2979 (2011).
 23. Cristovao, R. O. *et al.* Development and characterization of a novel l-asparaginase/MWCNT nanobioconjugate. *RSC Adv.* **10**, 31205–31213 (2020).
 24. Costa, J. B. *et al.* Enhanced biocatalytic sustainability of laccase by immobilization on functionalized carbon nanotubes/polysulfone membranes. *Chem. Eng. J.* **355**, 974–985 (2019).